KERNFORSCHUNGSANLAGE JÜLICH
GESELLSCHAFT MIT BESCHRÄNKTER HAFTUNG
Institut für Reaktorwerkstoffe

Pyrolysis of Methane by Microwaves
Part I

by

R. Avni, J. D. Winefordner and H. Nickel

Jül - 1188
April 1975

Als Manuskript gedruckt

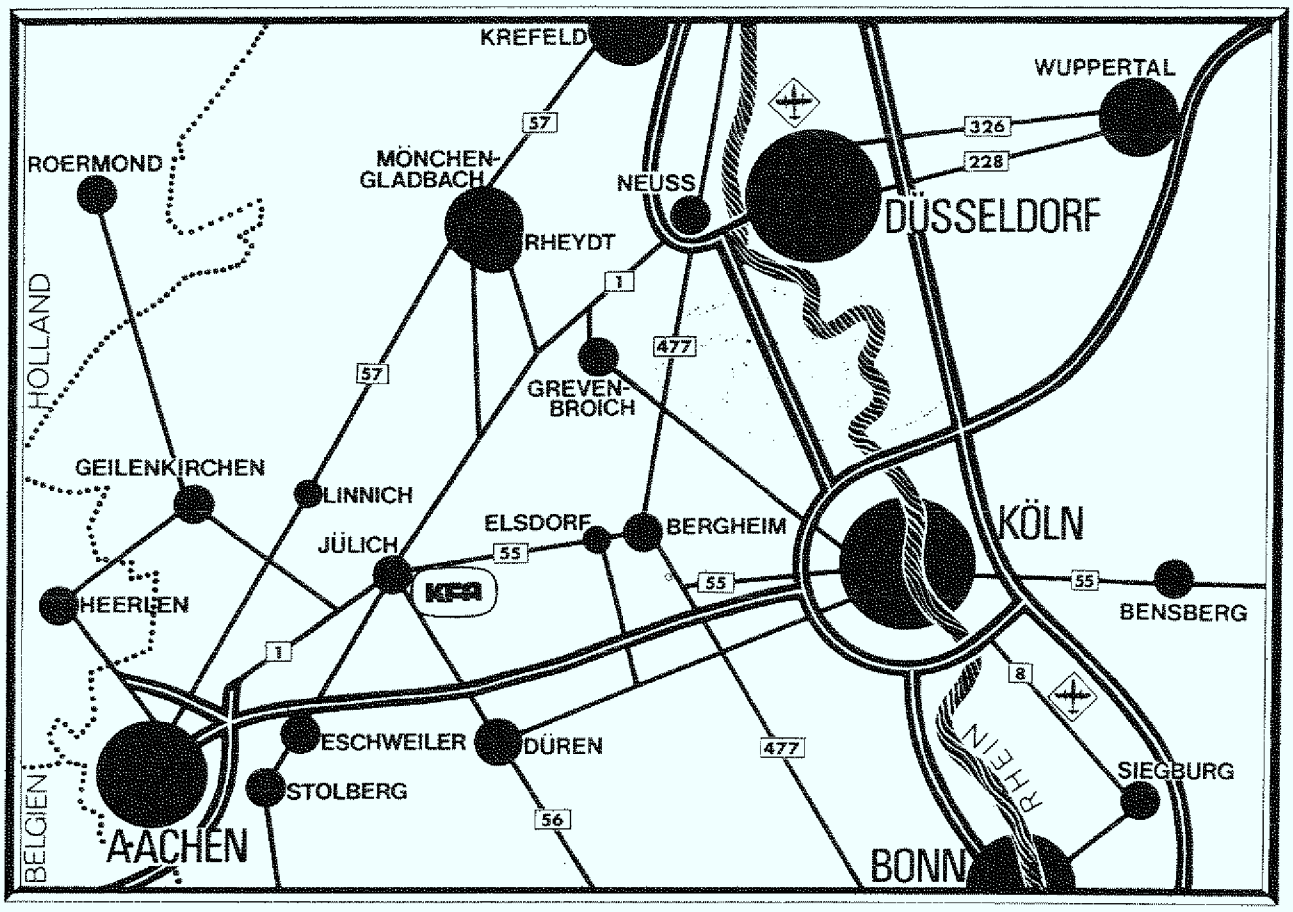

Berichte der Kernforschungsanlage Jülich - Nr. 1188
Institut für Reaktorwerkstoffe Jül - 1188 (Part I)

Dok.: Methane Pyrolysis - Microwave

Im Tausch zu beziehen durch: ZENTRALBIBLIOTHEK der Kernforschungsanlage Jülich GmbH, Jülich, Bundesrepublik Deutschland

Pyrolysis of Methane by Microwaves
Part I

by

R. Avni*, J. D. Winefordner** and H. Nickel***

* Israel Atomic Energy Commissions, N.R.C.-Negev, Beer Sheva, Israel
** Department of Chemistry, University of Florida, Gainesville, Fl., 32611 USA
*** Institut für Reaktorwerkstoffe, Kernforschungsanlage Jülich, W.-Germany

Kernforschungs-
anlage Jülich
GmbH IRW

JÜL-1188

April 1975

Pyrolysis of Methane by Microwaves

by

R. Avni*)
J.D. Winefordner**)
H. Nickel***)

ABSTRACT

The pyrolysis of methane and mixtures of argon-methane by microwaves (2450 MHz) was investigated.
The microwave plasma diagnostic study was performed using electrical probes, namely, the double floating probe technique. Parameters such as electric field strength and current densities were measured and from their relationship the electron temperature, electric conductivity, electron and ion densities were evaluated as function of gas pressure, microwave power input and distance of the probe from the microwave cavity. Various spectroscopic techniques were used for the measurement of temperatures in the microwave plasma; the "reversal temperature" by measuring the intensities of the electronic vibrational bands of CN and OH molecules and "rotational temperature" from the measured intensities of rotational OH lines. The "rotational" as well as the "reversal temperature" were found to be identical and this temperature was assumed to be the temperature of the gas in the microwave plasma.
Energy balance calculation, based upon the electrical energy input and thermal losses, were performed in order to determine if steady state conditions existed in the microwave plasma.
Emission and absorption spectroscopy were used for determining the active species formed in the pyrolysis of methane and also of mixtures of CH_4-Ar, by the microwave plasma.

*) Israel Atomic Energy Commissions, N.R.C.-Negev, Beer Sheva, Israel
**) Department of Chemistry, University of Florida, Gainesville, Fl., 32611 USA
***) Institut für Reaktorwerkstoffe, Kernforschungsanlage Jülich, W.-Germany

METHANPYROLYSE DURCH MIKROWELLEN

von

R. Avni
J.D. Winefordner
H. Nickel

KURZFASSUNG

Dieser Bericht enthält Untersuchungen zur Pyrolyse von Methan und Methan-Argon-Gemischen mittels Mikrowellenanregung (2450 MHz). Die Plasma-Diagnostik wurde mittels elektrischer Sonden, der sog. 'Doppelfluß-Sonden-Technik' durchgeführt. Dabei wurden die Parameter: elektrische Feldstärke und Stromdichte gemessen und aus ihrem Verhältnis Elektronentemperatur, elektrische Leitfähigkeit, Elektronen- und Ionendichte als Funktion des Gasdruckes, der Mikrowellen-Energie und des Sondenabstandes vom Resonator bestimmt. Durch Anwendung verschiedener spektroskopischer Methoden wurden folgende Temperaturwerte im Mikrowellen-Plasma bestimmt: 1. die 'Umkehrtemperatur' durch Messung der Intensitäten der Schwingungsbanden von CN- und OH-Molekülen, 2. die 'Rotationstemperatur' aus den gemessenen Intensitäten der OH-Rotationslinien. Es zeigte sich Übereinstimmung zwischen 'Rotations-' und 'Umkehr-Temperatur'; diese Temperatur wurde als Gastemperatur im Mikrowellen-Plasma angenommen.
Zur Prüfung der Frage, ob Gleichgewichtsbedingungen im Mikrowellen-Plasma existieren, wurden Berechnungen zur Energiebilanz durchgeführt; dabei wurden die zugeführte elektrische Energie und des weiteren die thermischen Verluste zugrundegelegt.
Die im Mikrowellen-Plasma während der Pyrolyse eines Methan- bzw. Methan-Argon-Gemisches sich bildenden Radikale wurden mit Emissions- bzw. Absorptions-Spektroskopie nachgewiesen.

C O N T E N T S

1. Introduction

The present investigation forms the first part of the study of the mechanism of pyrocarbon formation from the pyrolysis of methane. The microwave source was chosen based upon the similarity in temperature range as compared to the pyrocarbon formation in fluidized-bed which is the technique used for coating nuclear fuel kernels U- or U/Th-dicarbide or oxide with pyrocarbon.

The aim of this investigation is the study of electrical and optical parameters of the microwave discharge using electric probe and optical spectroscopy (emission and absorption) measurements.

The technique of electric probes for plasma diagnostics requires simple apparatus, although the theoretical analysis is complicated, there being no one universal method of interpretation. The probable reasons for this difficulty stems from the application of the method to a wide variety of different plasmas, such as flames[1-8], arc discharges[9,10], high frequency discharges[11,12], microwave cavities[13], and others[14-16]. As will be shown, the careful treatment of the double floating probes provides the evaluation of the following plasma variables: electric field (E); current density (j); electric conductivity (σ); electron and ion mobility(μ_e, μ_i); electron temperature (T_e); electron density (n_e); electron mean free path (λ_e); ion density (n_i); ionization degree (α); and ion diffusion coefficient (D_i).

The possibility that the gases in the microwave plasma are not in equilibrium indicate the difficulty in defining the temperature[6].

The line reversal method[6] was used to measure temperatures directly from the intensities of spectroscopic lines. This method can be applied to any spectral line terminating in a state near the ground state of atoms in any plasma. As shown in this work, the reversal temperature (T_r) is lower by at least one order of magnitude from the electron temperature (T_e), indicating the microwave plasma not to be in

local thermodynamic equilibrium. Due to this property of the microwave plasma, other techniques were used for evaluating temperatures. For example, the "excitation temperature" (T_{ex}) was evaluated from the measured intensity of two electronic excited vibrational bands of the cyanogen molecule [16a] namely in the $\Delta v=0$ and $\Delta v-1$ systems, i.e., these vibrational temperatures were designated as $(T_{ex})_v$. Moreover, the intensity of rotational lines of the 3064 Å vibrational system of the OH radical were used for the evaluation of the "excitation rotational temperature" $(T_{ex})_r$ [6].
As will be shown, an equality between T_r and $(T_{ex})_r$ was obtained resulting in the assumption that these temperatures represent gas temperatures.

Considering the energy input and its dissipation any non-LTE plasma can reach a steady-state. Under the steady-state condition, the reproducibility of a microwave plasma can be greatly improved.
The next-step, after determining the plasma diagnostics of the CH_4 and CH_4/Ar microwave plasmas, was the measurement of the species from the methane pyrolysis in emission and in absorption. Species like H, H_2, C, C_2, CH, and CH^+ were measured in emission while, CH_2, CH_3, C_2H_5, C_4H_2, C_2H_2 and C_6H_6 were measured by absorption using a Xe-arc (EIMAC) in continuum mode, as the light source for absorption. Both emission and absorption measurements were performed as a function of the gas pressure, microwave power, and the distance from the microwave cavity.

2. Theoretical considerations

2.1 Electric probes

When a potential is applied between a probe and the plasma, the probe current measured is the steady value that occurs when the ions and electrons have acquired their steady distribution within the electric field. Now, when the probe-

to-plasma potential difference changes, a time is required for the carriers to acquire their new equilibrium distribution, and so a finite time must elapse before the new probe current reaches a steady value. In other words, perturbations to an electrical probe current characteristic can be caused by fluctuations in plasma potential. The effect of these perturbations between probe and plasma can be reduced by using a double floating probe system[14,15].

In a floating double probe system, the net current drawn from the plasma in the EDL should be zero, i.e., the current flowing in the probe circuit is

$$i_s = i_{+1} + i_{e_1} = -(i_{+2} + i_{e_2}) \ldots \qquad (1)$$

where i_s is equal to the sum of the ion (i_+) and electron (i_e) currents to probe 1 and 2, respectively.

Increasing the applied voltage to the probes, a voltage is reached where the second probe becomes so negative that no electrons can reach it. As a result, the floating probe condition becomes[11,15]:

$$-i_{e_1} = i_{+1} + i_{+2} \qquad (2)$$

This condition is satisfied provided that the area of probes 1 and 2 are almost equal and that both probes are at a negative potential with respect to the plasma[11]. Assuming a Maxwellian distribution for the electron velocity, a probe radius much larger than the Debye length, and $T_e \geq T_i$, then the ion current density j_+ is approximately equal to[11-16]:

$$j_+ \approx 0.4\, n_i\, e \left(\frac{2kT_e}{m_+}\right)^{1/2} \ldots \qquad (3)$$

where j_+ is the random ion current density, A m^{-2},

n_i is the ion density, m^{-3}

m_+ is the ion mass, kg

$\left(\frac{2kT_e}{m_+}\right)^{1/2}$ is the kinetic ion velocity, ms^{-1}.

From the current-voltage plot, the electron temperature is determined as described elsewhere[11-13, 16].

The theoretical treatment of the double floating probe described in the literature[11-16] is based upon the assumption that the electron density in the plasma equals the ion density.

The electron current density to probe 1, j_{e_1}, A m^{-2}, is given by[11]:

$$j_{e_1} = -\frac{1}{4} e \left(\frac{8kT_e}{2\pi m_e}\right)^{1/2} n_e \exp (e V_{sh}/kT_e) \ldots \quad (4)$$

where m_e is the electron mass, kg, and V_{sh} is the sheath potential, V, which has a negative value. The sheath potential is derived by equalizing Eqs. 3 and 4, namely:

$$V_{sh} = -\left(\frac{kT_e}{2e}\right) \ln (0.44 \frac{m_i}{m_e}) \ldots \quad (5)$$

According to Swift and Schwar's theoretical treatment[11], for the symmetrical (equal surface) double floating probes Eq. 4 is inadequate for the evaluation of electron density because of the high negative value of the sheath potential. Only electrons in the high energy tail of the energy distribution will reach the probe. On the other hand, assuming ambipolar diffusion for ions and electrons in the microwave plasma, Allis and Rose[11a], derived the following relationship for the sheath potential:

$$V_{sh} = -1.08 \frac{D_e}{\mu_e} \ln (2.20 \frac{/u_e}{\mu_i}) - \frac{D_e}{3 \mu_e} \ldots \quad (6)$$

where D_e is the diffusion coefficient of electrons, $m^2 s^{-1}$ and μ_e and μ_i are the mobilitites of the electrons and ions, respectively, in $m^2 V^{-1} s^{-1}$.

A comparison of V_{sh} calculated by Eq. 5 and 6 shows that the sheath potential for Ar for example, is a factor two lower using Eq. 6 than the values determined by Eq. 5; therefore according to Eq. 6, less energetic electrons will be collected by the probe.

Another approach for the evaluation of the electron density is based on the assumption that the positive ion density in a microwave plasma is not equal to the electron density, merely because of electron affinity phenomena.

In our microwave plasma, the gas pressure is low. i.e., of the order to several mm Hg. At such a pressure, the electron mean free path is larger, allowing more collisions of electrons with the walls than in higher pressure plasmas. At such low pressures, the equality $n_i = n_e$ could be affected so that the real condition could be $n_i \neq n_e$. Therefore, it seems more appropriate to assume the electron flux is equal to the ion flux, i.e.:

$$\left(v_e\right)_d n_e = \left(v_i\right)_d n_i \quad \ldots \qquad (7)$$

where $\left(v_e\right)_d$ and $\left(v_i\right)_d$ are the drift velocities of the electrons and ions, respectively, in ms^{-1}. The drift velocity is used instead of the random velocity because of the electric field in the plasma of the EDL (see Appendix).

2.2 Electric field strength

The condition $n_i \neq n_e$ for a low pressure plasma will create a space charge which will cause an electric field in the plasma. The existence of this electric field can be tested experimentally. In Figure 1, the set up is shown for measuring the electric field strength, E, between two tungsten electrodes. It should be proved, however, that the voltage between the two probes is:

i) not influenced by the wire material (W or Pt) and by the diameter (cross-section) of the wire, i.e., the wire emissivity is not measured instead of voltage; and

ii) the voltage values are influenced by the gas pressure, i.e., lower value at higher pressures.

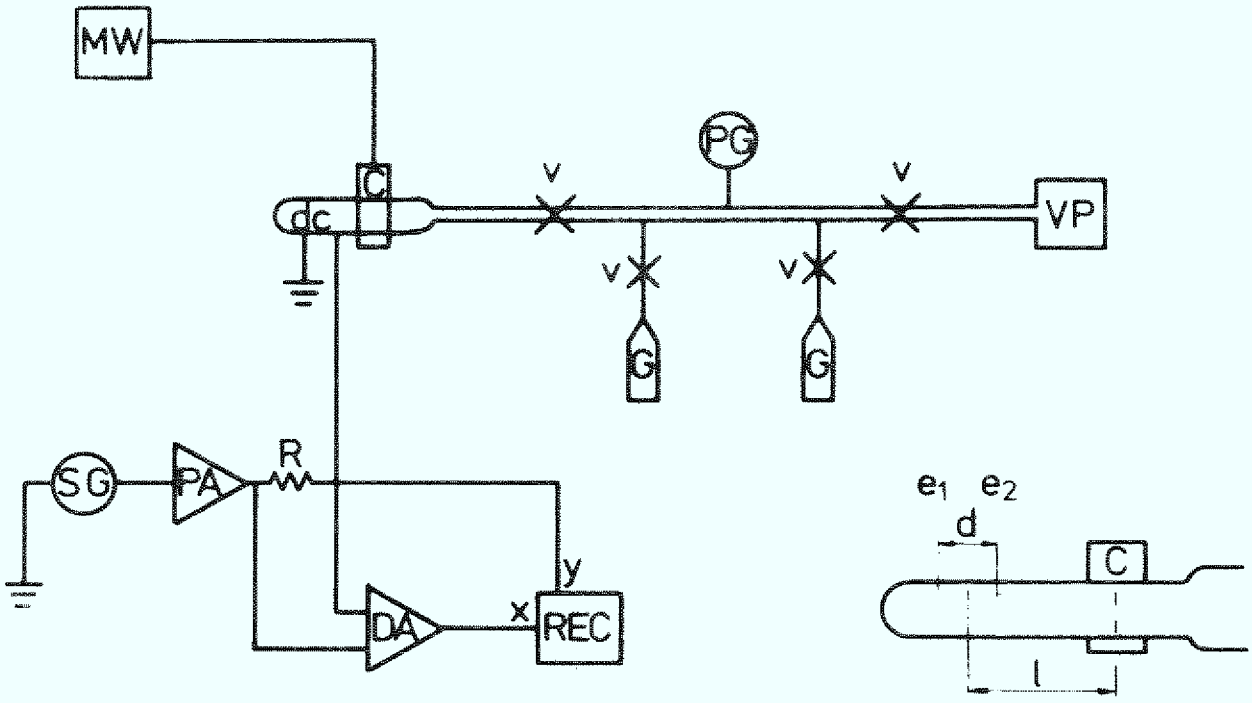

Fig. 1: Instrumental Setup for Floating Durable Probe Measurements

C = Microwave Cavity (Evenson Type)
DA= Differential Amplifier
dc= Discharge Cell (tube diameter 11 mm o.d.)
$e_1 e_2$ = W probes
G = Gas Supply
MW= Microwave Power Supply (245o M Hz, 2oo W)
PA= Power Amplifier (± 5o V)
PG= Pressure Gauge
R = Resistor (1oo Ω)
REC = X-Y Recorder
SG= Sweep Generator
V = Valves
VP= Vacuum Pump
d = distance between probes (d varies from ≈1 to 5 mm)
l = distance between center of cavity and midpoint between electrodes (l varies from 1o to 25 mm)

The voltage data for the present studies in Table 1 fulfill the above two requirements.

The plasma voltage between two points can be obtained also from the current-voltage plot of the double floating probe; it is the value at the intersection of the current-voltage curve with the voltage abscissa (at zero current).

Pressure	E_1 V cm^{-1}			E_2 V cm^{-1}	
Torr	W wires ϕ0.6 cm	w wires ϕ1.2 mm	Pt wires ϕ0.5 cm	w wires ϕ=0.6 cm	Pt wires ϕ=0.5 cm
1.0	18.0	18.0	16.6	16.6	20.0
6.0	12.0	13.0	12.0	14.0	12.0
10.0	8.0	6.6	7.5	6.6	5.5

E_1 = values obtained by a voltmeter - rel. st. dev. $\pm$ 2o %.
E_2 = values obtained from the double floating technique - rel. st. dev. $\pm$ 3o %.

Table 1: Electric Field with Wire Material and Cross Section. 12o W MW Power. Distance between electrodes o,35 cm; Distance from antenna's cavity - 1.3 cm.

2.3 Other electric variables

From the current density and the electric field strength values obtained from the current-voltage plot of the double floating probes, electric parameters such as electric conductivity (σ), electron density (n_e), ion drift velocity $(v_i)_d$, and ion density (n_i) can be derived as described by Francis[19], Finkelnburg and Maecker[1o], Boumans[2o], and others[21,22].

From the relationship of current density, j, and electric field strength, E, one obtains σ , the electric conductivity, in $\Omega^{-1}m^{-1}$:

$$\sigma = j_e/E \qquad (8)$$

where j and E are expressed in A m^{-2} and V m^{-1}, respectively.

Assuming the current in the EDLs plasma is carried exclusively by the electrons, then the electric conductivity is defined as

$$\sigma = e\,\mu_e n_e \quad \ldots \qquad (9)$$

where e is the electron charge, in C, μ_e is the electron mobility, in $m^2 v^{-1} s^{-1}$, and n_e is the electron density, in m^{-3}. In using equation 9 for the n_e calculation, one needs the value of μ_e. The electron mobility is defined as the electron drift velocity $(v_e)_d$, in ms^{-1}, in an electric field of V/r, i.e.:

$$\mu_e = (v_e)_d / E \qquad (10)$$

The electron drift velocity in various gases is known[22-25] to be a function of the electric field (E) and gas pressure. From the μ_e and T_e values, the electron mean free path (λ_e, in m) can be calculated from:

$$\lambda_e = \mu_e \sqrt{T_e} / 2.61 \cdot 10^9 \qquad (11)$$

From equations 8-10, the current density of the probes is given by: (taking into account $j_e = -2j_i$)

$$j_e = e n_e (v_e)_d \approx 0.8\, n_i e \left(\frac{2kT_e}{m_+} \right)^{1/2} \ldots \qquad (12)$$

and from Eq. 7 and 12, the final result for the ion drift velocity $(v_i)_d$ is:

$$(v_i)_d \approx 0.8 \left(\frac{2kT_e}{m_+} \right)^{1/2} \quad \ldots \qquad (13)$$

From the product $n_i (v_i)_d$ obtained from equation 7 and $(v_i)_d$ being calculated from equation 13, n_i can be obtained directly. The above equations are adequate for the presence of only one gas in the EDL, for example, argon, helium, or nitrogen. For mixtures of gases like Ar and N_2 with different ionization potentials and degree of ionization between them, Eq. 3 should be transformed with regard to m_+.

2.4 Temperature

(i) "Reversal Temperature"

The spectral line 5350 Å ($6^2P_{3/2}$ - $7S_{1/2}$) of thalium atom was chosen; the lower level has an energy of 0.96 eV and the upper level has an energy of 3.3 eV. This line was reversed by a calibrated tungsten ribbon lamp, and the "reversal temperature" was measured in the usual manner[6,27,28]. The $6^2P_{3/2}$ level is the metastable level of Tl(I). If this level is solely populated by cascade transitions from the upper states, as a result of inelastic collision with high energy electrons, or with excited heavier particles (CH_4; CH_3; CH_2, or CH, for example), then the 5350 Å cannot be reversed because the $6^2P_{3/2}$ is not sufficiently populated, particles being spread in energy over various states of Tl I, according to the lifetimes of the states. Because the mean kinetic energy of the electrons in a low pressure microwave plasma is of the order of 4 eV, one may assume that the 0.96 eV level is not preferentially populated by collision with these electrons. Therefore one may assume that the population of the $6^2P_{3/2}$ state of Tl is mainly determined as a result of the gas temperature in the microwave plasma.

A concentration range of 0.1 - 1 % (atom %) of Tl (as TlCl) in CH_4 and CH_4 + Ar was introduced into the tube.

(ii) "Excitation temperatures $(T_{ex})_r$ and $(T_{ex})_v$"

a. Rotational temperature (OH). The temperature was determined from the distribution of intensities among the lines of the rotational fine structure of a band spectrum. The intensity I, of a rotational line of a vibrational band in an electronic transition is given[6]:

$$I_r = C(gA)_r \nu^4 \exp(-E_r/kT) \quad \ldots \qquad (14)$$

where C is a constant which is the source for all rotational lines of the same bond, $(gA)_r$ is the statistical weight factor times the rotational transition probability, ν is the wavenummer, E_r is the rotational energy of the initial state, k is

the Boltzmann constant and T is the gas temperature. The transition probabilities values were taken from the data published by Dieke and Crosswhite[26] for the OH band at 3064 Å. The spectrum of OH present in the CH_4 or CH_4 + Ar microwave plasma is a result of the oxygen impurities in either CH_4 or Ar, while hydrogen is obtained from the pyrolysis of the methane. The method for the temperature determination is the "plotting method". Eq. 14 can be rewritten in its logarithmic form i.e.:

$$\log_e I_r = \log_e C + \log_e(gA\nu^4) - 625\ E_r/T \ldots \qquad (15)$$

in which E_r is given in kK. We plot $(\log_e I_r - \log_e(gA\nu^4)$ against E_r, a straight line is obtained with a slope - 1/T. This method is subject to errors due to self-absorption, but because it makes use of 5 rotational lines (with unequal self-absorption) and small concentration of the OH radical, no strong self-absorption effect was detected.

b. Vibrational Temperature (CN). The cyanogen, CN, molecule is formed in the CH_4 microwave plasma from the N_2 impurities in methane and from the carbon resulting from the methane pyrolysis. The 3883 Å vibration sequence, ($\Delta v=0$), is the only one easily detected because of the small concentration of the CN in the microwave plasma. The other sequences (i.e. $\Delta v = -1$ and $\Delta v = 1$) although obtained are too weak to be measured accurately. The method applied for the vibrational temperature was described by Smit[16a], in which the intensity ratios of two band heads, i.e. 0-0 3883 Å and 1-1 3872 Å, were measured:

$$\frac{I_{(0-0)}}{I_{(1-1)}} = \frac{(\nu^4 gA)_{0-0}}{(\nu^4 gA)_{1-1}} \exp\,(E_v/kT) \ldots \qquad (16)$$

where E_v is the difference in energy of the excited vibrational bands. The transition probabilities used were those given by Smit[16a].

Both the OH and the CN radicals require excitation energies of about 4 eV and 3 eV, respectively. This energy may be supplied by the heating effect of the microwave (gas temperature) or more probably by inelastic collisions with electrons. As will be shown, the electrons in the microwave plasma have kinetic energies greater than those required for the electronic excitation of OH and CN.
Therefore, the difficulty in such a system is to assign the measured "excitation temperature" as the gas temperature. Based upon the equality between the reversal and the rotational temperature, we will assume in this work that it does represent the gas temperature.

2.5 Energy balance

For energy balance considerations, the work of Elenbaas[17], Heller[18], Roes[21], and others[22] for dc arc plasma will be utilized in the present studies.
The energy balance is expressed as the equality of energy input and the energy loss per unit volume and time.
Neglecting energy loss by radiation compared to losses by thermal conduction, Elenbaas[17] and Heller[18] formulated the following equation for systems under steady state conditions,

$$\text{div} (\varrho \, \text{grad} \, T) + jE = 0, \ldots \qquad (17)$$

where ϱ is the thermal conductivity, in J $s^{-1}m^{-1}K^{-1}$, and T the absolute temperature, in K.
For a cylindrical symmetry (z,r) of the microwave plasma, the above equation will take the following form after integration:

$$-r\varrho \frac{dT}{dr} = \int_0^r j \, Er \, dr, \ldots \qquad (18)$$

with dT/dr = 0 as boundary condition along the z axis, where r = 0. Equation 18 shows that the electric energy dissipation in a cylinder of unit height (dz = 1) is equal to the heat

leaving this cylinder in unit time. If only the plasma between the double probes is considered for which the values of E and j are constant, then equation 18 can be rewritten as:

$$jE = -\frac{\varrho}{r}\frac{dT}{dr}, \quad \ldots \qquad (19)$$

Substituting the j value from equation 9, equation 19 takes the form:

$$\bar{n}_e = -\frac{2\rho}{e\,\mu_e r E^2}\frac{dT}{dr}, \quad \ldots \qquad (2o)$$

where $\bar{n}_e$ represents the average electron density for the region considered. Introducing the temperature gradient as obtained from the rotational spectrum of OH using the line reversal method, $\bar{n}_e$ can be calculated. The agreement in $\bar{n}_e$ values with those obtained by the double probe floating method (n_e) describe the steady state conditions of the plasma in the microwave discharge.

2.6 Absorption spectroscopy of radicals formed in the microwave plasma

The aim of the absorption measurement is to detect and evaluate other radicals such as CH_2, CH_3, C_2H_2, etc., which may well be produced in the pyrolysis process. Absorption spectroscopy is the spectroscopic technique used for achieving the aim. Moreover, formation of molecules such as C_2H_2, C_4H_2, C_6H_6 or with higher carbon numbers, may also be produced in the pyrolysis process[3o] and detected by absorption spectroscopy.

Herzberg[31], Gaydon[32], and others[33-35] using absorption spectroscopy did obtain and partially classify the absorption spectrum of CH_2, CH_2^+, CH_3^+, and C_2H_5 radicals in flash photolysis (diazomethane, methyl iodide and mercury dimethyl) or low pressure flames of methane, methyl ether or acetone.

Based on their data, various absorption techniques were used in the present investigation in order to evaluate the presence of above radicals and molecules in the pyrolysis of CH_4 by microwaves.

In absorption spectroscopy, the important factor which should be taken into account is the lifetime of such radicals and molecules in their ground or excited states. Herzberg[35], for example, estimated the lifetime of CH_2 and CH_3 radicals as being in the order of 5o ms and 5o μs, respectively. Experimentally, measurements can be achieved in a flow system in which the radical is continuously-produced, like in a flame[32], for example, or in a non-flow system provided the absorption measurement is made in the μs region, i.e., one order of magnitude faster than the shortest lifetime of the any radical or molecule.

Various systems were investigated in order to obtain the suitable experimental set up for the absorption spectra. The following systems were investigated:

i) A non-flow system in which methane or mixtures of methane with argon were introduced at various pressures and the absorption of the species measured within the microwave plasma.

ii) A non-flow system similar with the above (i) in which the absorption spectra was measured in the afterglow region of the microwave plasma.

iii) A flow system in which various flow of methane were produced at several torr pressure, and the absorption spectra measured within the microwave plasma.

Using multiple optical passes through the region of interest, it was thought that one of the above systems would be the most adequate for the absorption measurements.

Another factor of interest in the absorption spectra is the weak spectral character of the absorption band of most radicals. A general feature of radicals such as CH_2, CH_3, C_2H_5, C_4H_2, or molecules such as C_2H_2 and C_6H_6 is that they show diffuse, weak and non-well-defined band heads[36].

Moreover, some radicals and molecules show uncertainty with regard to their assignments. For example, the head group at 4o5o Å which was assigned to CH_2, belongs probably to C_3 radical, or 2264 and 2367 Å assigned to CH^+, belongs to HgH^+ [36] and the 2242 and 2228 Å are provisionally assigned to C_2H_5 radical[32,35].

3. Experimental

3.1 Diagnostics

The equipment used is indicated in Fig. 1. The vacuum system was pumped down to $\sim 1o^{-2}$ torr and flushed several times with the appropriate gas before measurement (CH_4, prepurified, 99.998%; He high purity, 99.995%; Ar, high purity 99.995%). The discharge cell (insert of Fig. 1), was constructed of Pyrex, so that the tungsten wire probe (normally o.6 mm diameter) could be sealed with canary glass. The probes were connected to the electrical system via crimped connectors for good electrical contact. The smaller (11 mm od) diameter end was placed in the cavity, with the distance between the electrodes and the center of the cavity being variable. The larger (16 mm od) diameter end was required for connection to the vacuum system. Compressed air was passed through the cavity both to cool the cavity and to avoid overheating and melting the pyrex. For the determination of reversal temperature, the smaller diameter end was made of Vycor, with a graded-seal to the pyrex portion. A tungsten ribbon filament lamp was used to measure the reversal temperature with a o.35 m monochromator and photomultiplier tube. As the lamp was calibrated in spectral radiance (by Eppley Laboratories), the data of Vujnović[28] was used to obtain the temperature of the filament vs lamp current. The 535o Å line of Tl was used to measure the reversal temperature (with 2.o μg Tl as chloride in the discharge tube).

Current-voltage curves were recorded automatically by applying a sweep voltage to the electrode and measuring the voltage drop through the series resistor with a differential amplifier, the output of which was used as the Y drive of the X-Y recorder. Sweep rates were ~ 5 Vs^{-1}. One probe was grounded, but the system still involved floating the double probes as the plasma was floating with respect to ground. This was confirmed by using a system similar to the above, except that instead of grounding the reference probe to electrical or earth ground as above, the reference probe was used as signal ground, and all instruments were floated so that signal ground was isolated from earth ground. Because both cases gave identical V-i curves, the simpler system was used for experimental measurements. The voltage measured at zero current was shown to be the DC potential difference between the two probes by independent measurement of the voltage difference between the two probes, using a VTVM, for several different probes, as indicated in Table 1.
The DC potential difference between the probes divided by the distance d between the electrodes gives the plasma's electric field strength, E. The displacement of the probes in the cavity with respect to the cavity position gives the electric field strength gradient in the plasma (dE/dl).
The "excitation temperature" were measured by a 3.4 m Ebert J. Ash spectrograph using spectrographic plates. The spectrograph was used in order to obtain the spectral resolution needed for the rotational spectrum of OH. The "Ebert spectrograph" was equipped with a grating of 1200 lines/mm giving a reciprocal dispersion of 2.5 Å/mm. The OH and CN spectra were measured by means of densitometer.

3.2 Absorption

Fig. 2-4 show the three different optical setups for the absorption measurements. The following items are common to the three optical setups:

i) The light source for the absorption is a Xe arc lamp made by EIMAC, Model 15o x 8S (EIMAC, Division of Varian, San Carlos, CA) delivering 15o W in a continuum mode. The illuminator power supply is a EIMAC Model P25oS-2.

ii) The light from the Xe lamp is chopped by a P.A.R. mechanical chopper Model 125, (Princetown Applied Research,NJ).

iii) The microwave cavity is a Evenson type which is powered by a 245o MHz microwave power generator Microtron 2oo made by Electro Medical Supplies, Wantage, Berkshire, England, operating in a continuum mode.

iv) The absorption spectra are measured by a o.5 m Ebert type scanning monochromator made by Jarrel-Ash. The detection system consisted of a RCA photomultiplier P-21, a Jarrel-Ash high voltage power supply, an Ithaco lock-in amplifier Model 353 (Ithaco, Inc. Ithaco, NY) and a Texas Instruments Recorder Model Servo Riter II (Texas Instruments, Attelboro, MS).

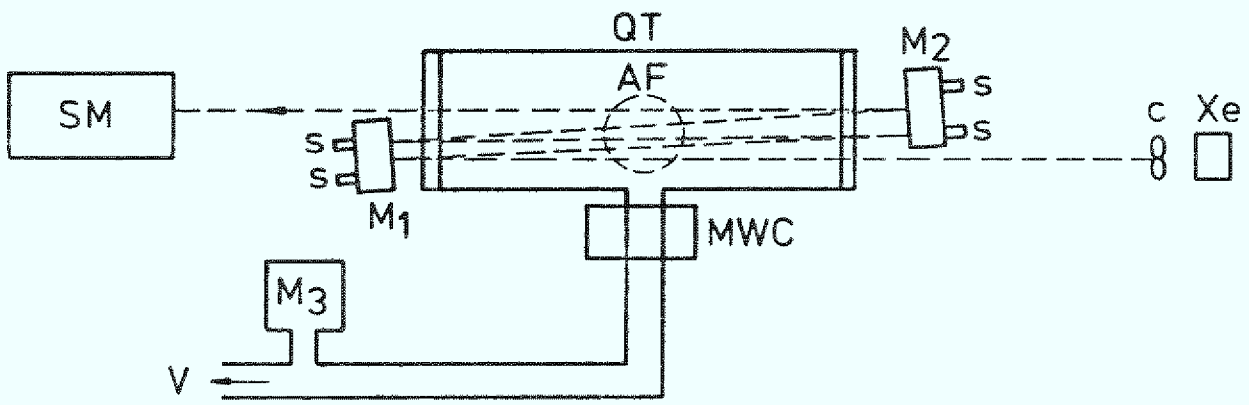

Fig. 2: The afterglow system.
Xe=Xe lamp; c=chopper; M_1=mirror; M_2=mirror; s=tilting screws; QT=quartz tube; AF=Afterglow region; SM=scanning monochromator; MWC=microwave cavity; M_3=manometer; V=to vacuum pump and fitting for gas introduction.

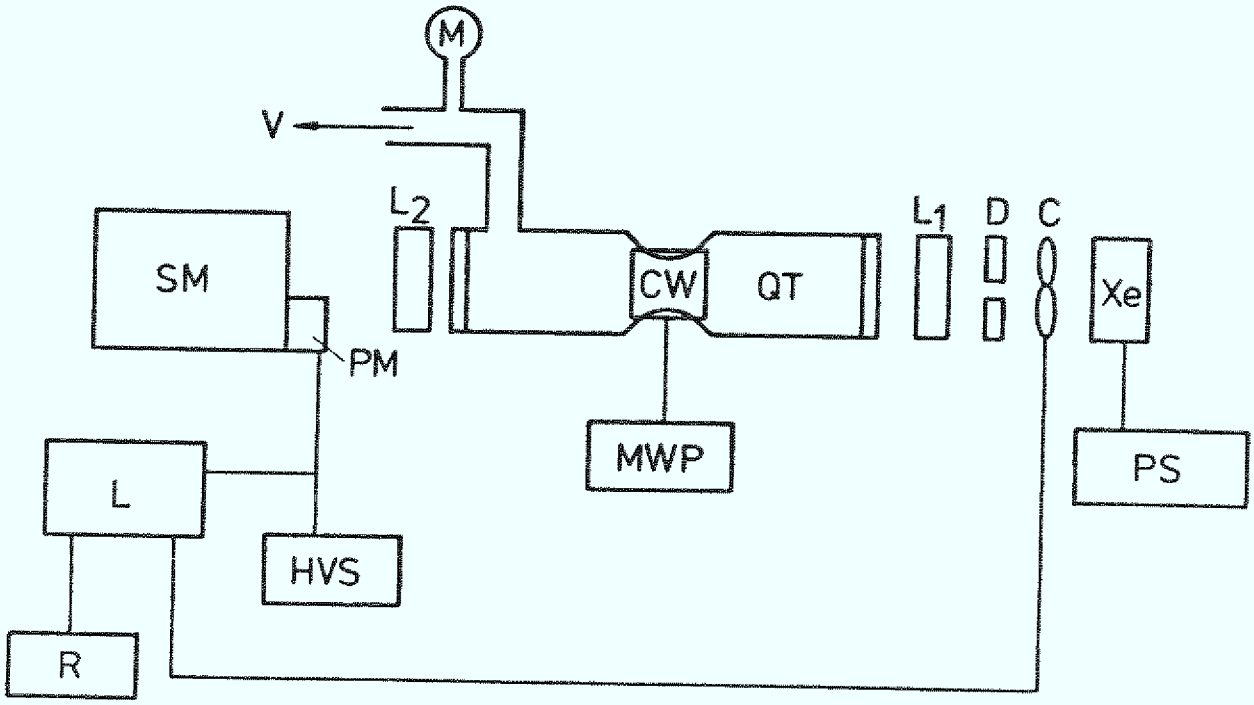

Fig. 3: Blockdiagram of the non flow system.
Xe=Xe lamp; PS=power supply to Xe lampe; C=chopper; D=diaphragm; L_1,L_2=quartz lenses; QT=quartz tube; CW=microwave cavity; MWP=microwave power generator; M=manometer; V=to vacuum pump system; SM=scanning monochromator; PM=photomultiplier; HVS=high voltage supply; L=lock in amplifier; R=recorder

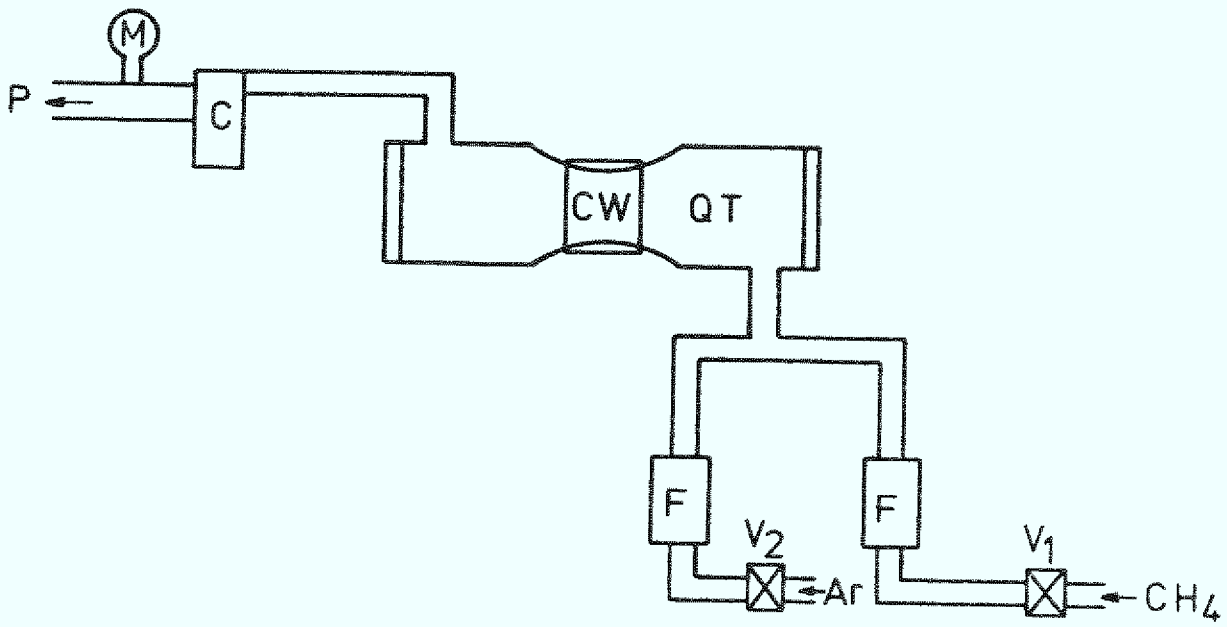

Fig. 4: Flow system.

V_1,V_2=Admittance valves; F=flowmeters; CW=microwave cavity; C=cold trap; M=manometer; P=to vacuum-pump-System; QT=quartz tube

Fig. 2 shows the setup for measuring the absorption spectrum in the afterglow region. At each side of the quartz tube a mirror is placed in such a way that the light from the Xe lamp will have 5 passages through the same portion of the afterglow region before reaching the monochromator.

The distance between the microwave cavity and the afterglow region is about 2 cm. The particles formed in the cavity have to travel this distance in order to be measured in absorption. A radical with a lifetime of 1o μs, for example, should travel his distance with a velocity of 2 x $1o^3$ m s^{-1} in order to be measured in absorption. At gas pressures of several torr and a temperature of about 3oo^{o}C at 2 cm distance from the cavity, the mean random velocity of the particle is given by $v = (3kT/m)^{1/2}$. For example, the CH_3 radical under such conditions has a mean random velocity of $\sim 3 \times 1o^3$ m s^{-1}. In other words, molecules with life time shorter than 1o μs cannot be detected efficiently in absorption in such a system.

Figs. 3 and 4 show the system for measuring the absorption spectrum through the microwave plasma of CH_4. The CH_4 or the mixtures CH_4 + Ar are stationary in the system describe in Fig. 2, at pressures ranging from o.5 to 1o torr, while in the system described in Fig. 3 a continuous flow of CH_4 was passed through the microwave cavity each at constant pressure ranging from o.5 to 5 torr. In both systems, the light from the Xe lamp passing through the CH_4 plasma measured the absorption independently of their life time. The difference between the system described in Figs. 2 and 3 consisted in the rate of formation of the radicals or the molecules of interest; in the flow system, the rate of formation can be assumed constant with time, while in the stationary system, this rate will vary with time.

The spectral range scanned for the three systems was from 2ooo-34oo Å only. Almost all the spectral information needed for the radicals and some molecules like C_2H_2 and C_6H_6 can be found in this region[35].

4. Results and discussion

4.1 Diagnostics

4.1.1 Electric field strength (E)

The electric field strength was measured separately in each gas as well in their mixtures. Fig. 5 shows the measured E values. The space charge in the microwave plasma develops the electrostatic field, which is greater in Ar than in CH_4 at various pressures.

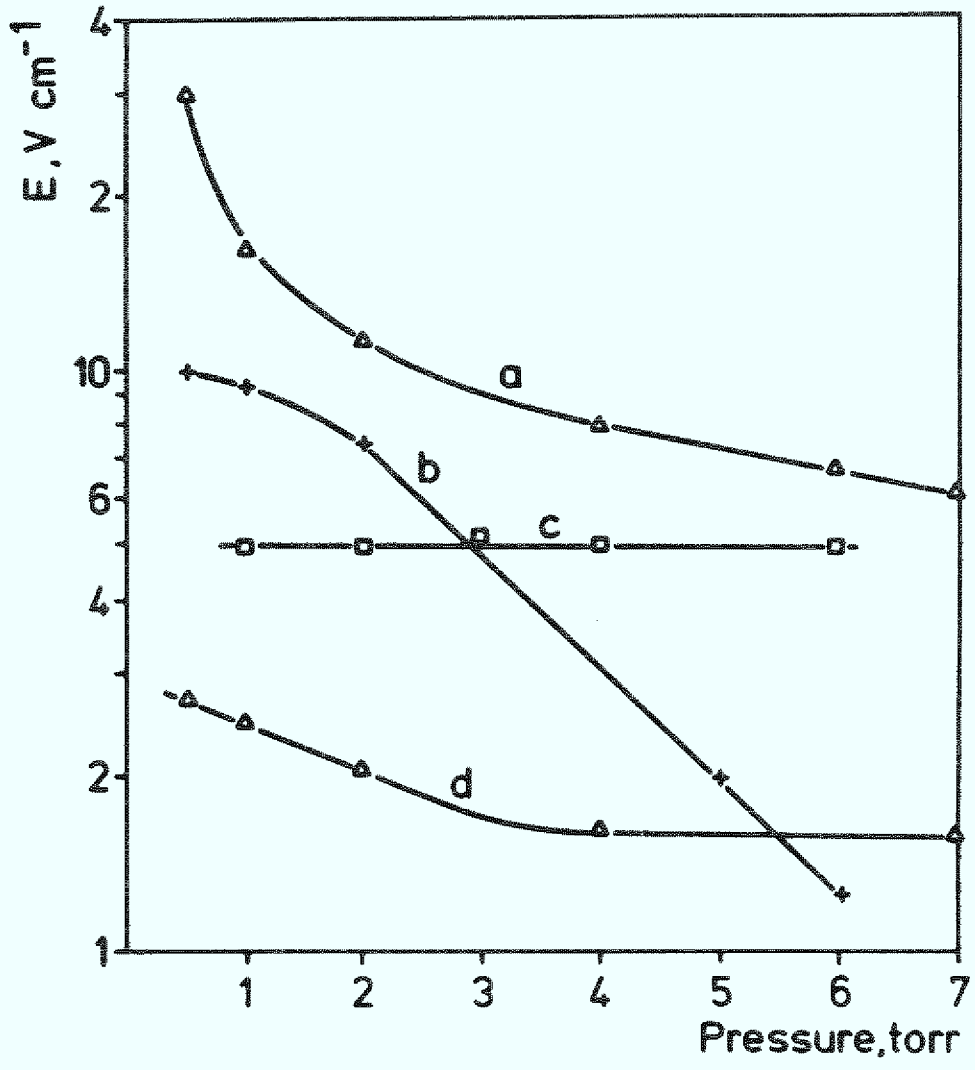

Fig. 5: Electric field strength vs. pressure.
d = 0.6 cm; l = 1.3 cm; 120 W.
a=Ar; b=CH_4; c=Ar + varying CH_4; d=CH_4 + varying Ar.

This effect is connected to higher interaction of electrons and ions in the methane gas as compared with argon. It will be discussed in detail at 4.1.3. The addition of CH_4 to Ar or vice versa has a two-fold effect: i) it decreases the electric field values as compared with the respective pure gases up to a pressure of≈3 torr; and ii) the E values are almost constant with respect to pressures > 3 torr. In other words, comparing with the pure gases, the space charge in the plasma is lowered and almost constant at different pressures. The marked effect on the electric field values in gaseous mixtures is due to the position of the double probes with respect to the distance from the antenna. Fig. 6 shows the electric field gradient within the plasma from o.2 to 1.6 cm away from the microwave antenna.

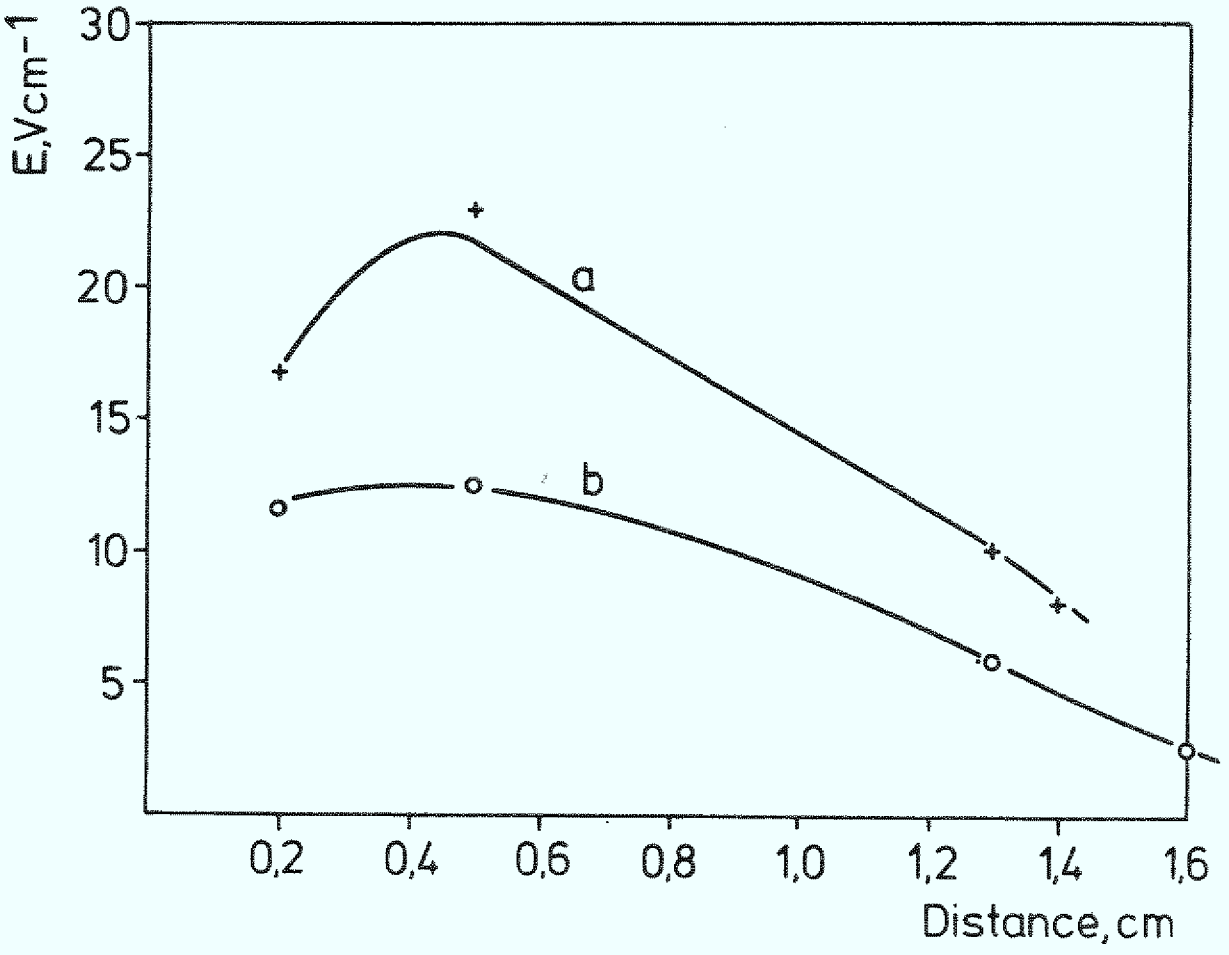

Fig. 6: Electric field strength vs. distance from the cavity center.
d = o.6 cm; 75-12o W
a)CH_4 2 torr; b)Ar 4 torr + CH_4 2 torr.

As the probes approach the cavity, higher E values result. The increase in E values nearer the cavity is a result of a higher electron temperature T_e, which increases the electron drift velocity $(v_e)d$, leaving the ion drift velocity $(v_i)d$ almost constant (see Table 3). In other words, the space charge increases, nearer to the center of the cavity.

4.1.2 Electron temperature (T_e), reversal (T_r) and rotational $(T_{ex})_r$ temperatures

Fig. 7 shows the electron temperature, T_e, values as measured from the current voltage plot of the floating double probe.

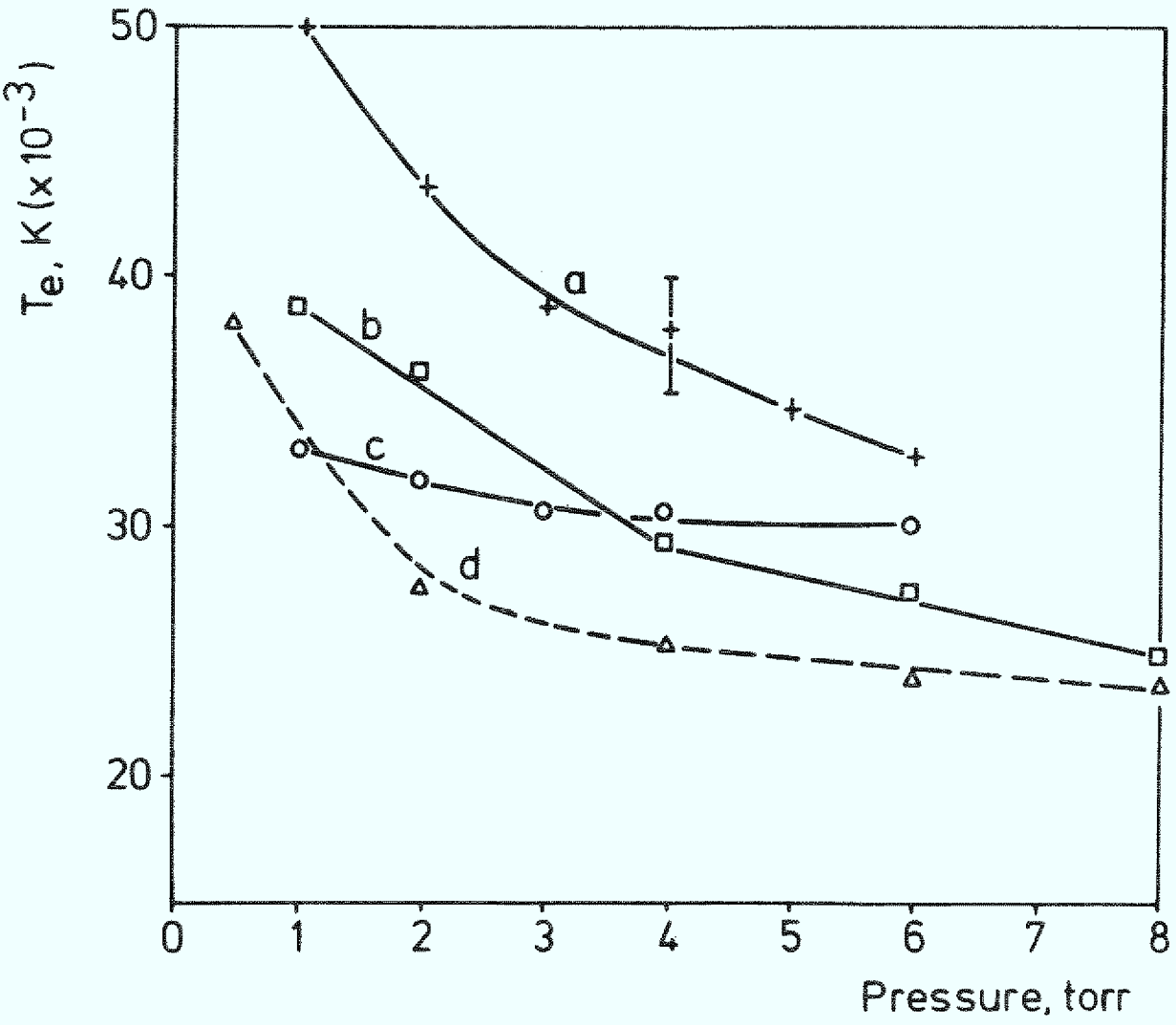

Fig. 7: Electron temperature vs. pressure.
d = 0.6 cm; l = 1.3 cm; 120 W.
a=CH_4; b=Ar; c=Ar + varying CH_4; d=CH_4 + varying Ar.

In the plasma of each gas, the electron temperature in CH_4 is higher than in Ar, decreasing as their pressure increases. Addition of argon to a constant methane pressure, lowers the electron temperature reaching a constant value above 3 torr of argon. The addition of CH_4 to a constant pressure of Ar increases T_e as compared to the previous conditions, keeping it constant with CH_4 pressure above 1.o torr CH_4. The reasons for $(T_e)_{CH_4} > (T_e)_{Ar}$ are rather complex and depend greatly on factors such as: the electron velocity distribution, electron conductivity (see Fig. 8) and on the exothermic reactions in the pyrolysis of methane.

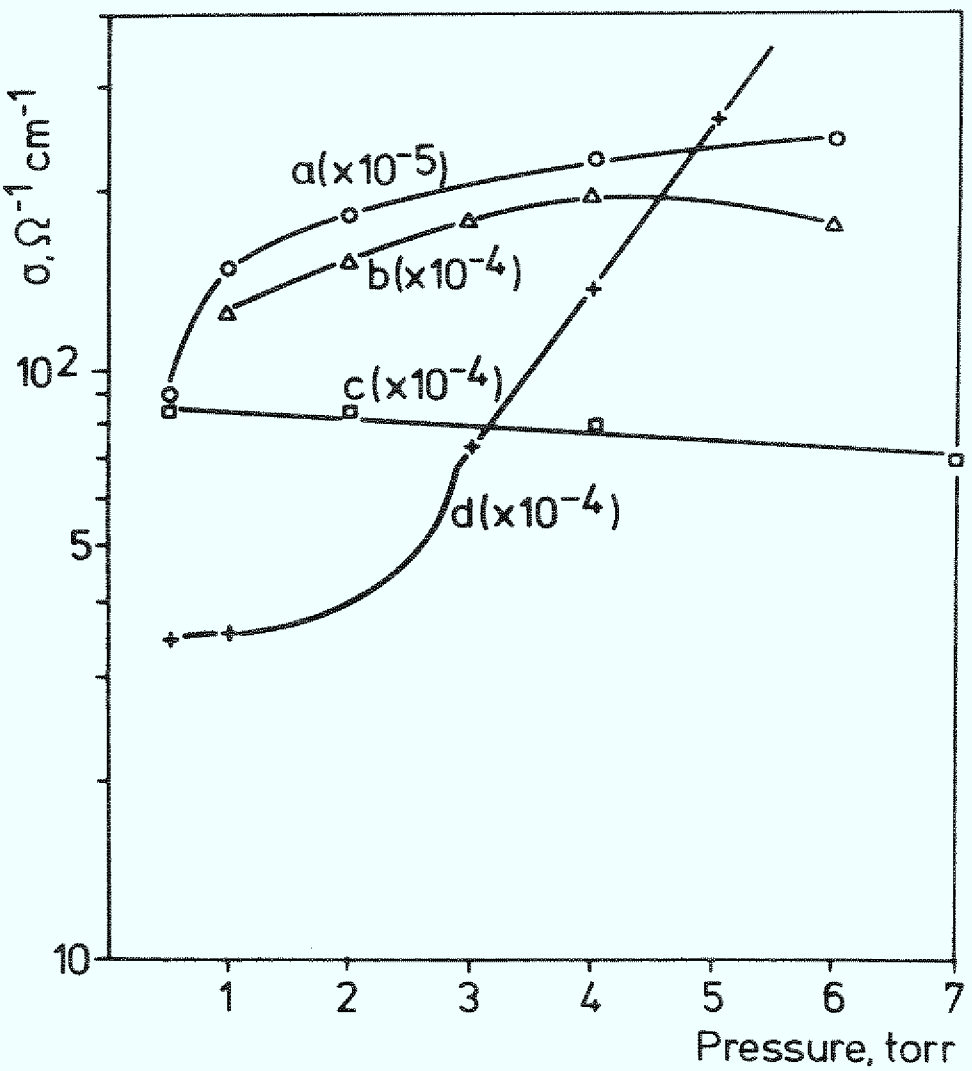

Fig. 8: Electric conductivity vs. pressure.
a=Ar; b=4 torr + varying CH_4;
c=2 torr CH_4 + varying Ar; d=CH_4.

Fig. 9 shows the "reversal temperature" measured with thallium atoms while Fig. 1o shows the rotational temperature (measured with the OH radical) at several gas pressure. The OH was introduced in the argon by bubbling the gas through water. The higher temperature values T_r and $(T_{ex})_r$ in CH_4, as compared with those in Ar up to 4.o torr, indicate that exothermic chemical reactions occur in the pyrolysis of methane. In Table 2, the electron random velocity $\bar{v}_e$ and the electron drift velocity $(v_e)_d$ are given. The result by which $\bar{v}_e > (v_e)_d$ indicates that the microwave source results in a plasma which is more thermal than electric. Based on that effect as well as on the description given in section 2.4 (i) of this report, the assumption that both T_r and $(T_{ex})_r$ represent also the

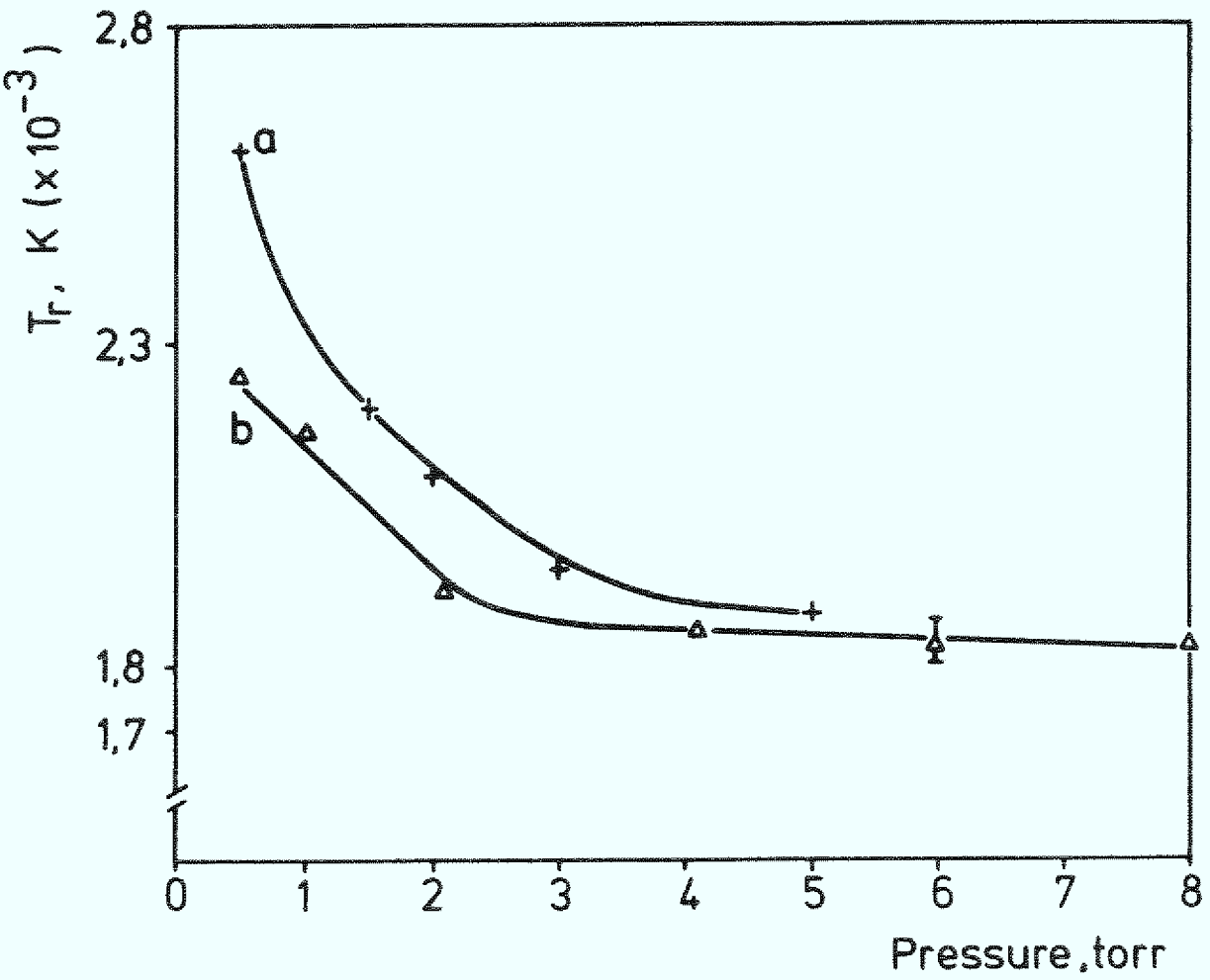

Fig. 9: "Line reversal temperature" vs. pressure. d = o.6 cm; l = o.5 cm; microwave Power 12o W. a=CH_4; b=Ar.

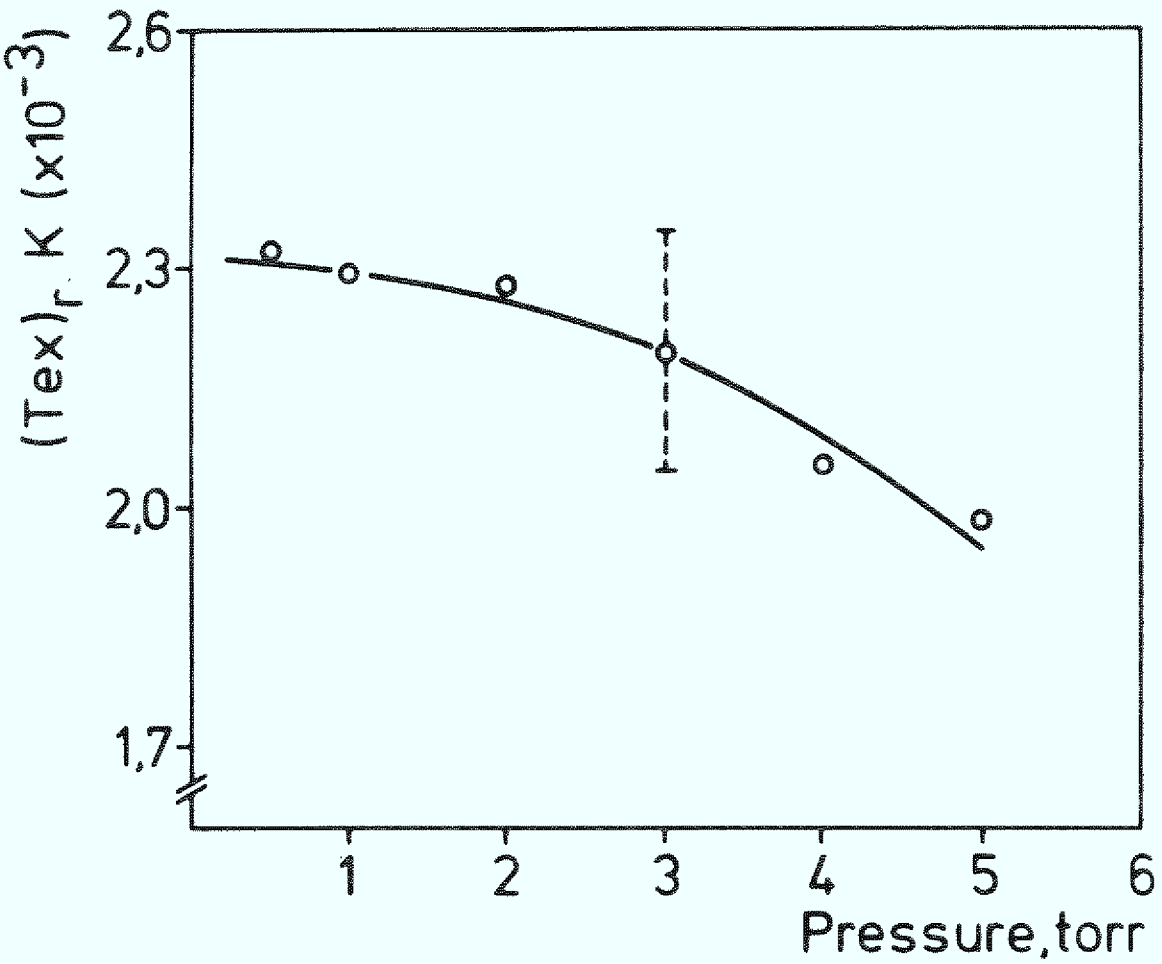

Fig. 1o: "Rotational temperature" (OH) vs. CH_4 pressure. 1.o torr; microwave power 12o W; near cavity center.

gas temperature in the microwave cavity is in part justified. A comparison between both the "reversal" and "rotation" temperature values to the electron temperature values indicates conclusively the non-LTE behaviour of the microwave plasma, i.e., $T_e > T_r \simeq (T_{ex})_r$ by more than one order of magnitude (see Fig. 7).

Fig. 11 shows the T_r and $(T_{ex})_r$ as function of the distance from the center of the microwave cavity in a methane plasma. A drop of about 1ooo K was obtained for the "reversal" and the "rotational" temperatures at 4 cm distance from the center of the microwave. The electron temperature also drops to the same 4 cm distance. Nevertheless at 4 cm distance from the center of the microwave

CH_4				Ar			
P Torr	T K	$\bar{v}_e \times 10^7$ cm sec^{-1}	$(\bar{v}_e)_{drift} \times 10^6$ cm sec^{-1}	P Torr	T K	$\bar{v}_e \times 10^7$ cm sec^{-1}	$(\bar{v}_e)_{drift} \times 10^6$ cm sec^{-1}
0.5	2800	3.56	5.3	0.5	2450	3.35	7.0
1.0	2500	3.40	4.0	1.0	2350	3.30	3.0
2.0	2300	3.30	1.4	2.0	2100	3.10	1.8
4.0	2100	3.10	1.0	4.0	2050	3.04	0.9
6.0	2080	3.06	0.06	6.0	2050	3.04	0.6
				8.0	2050	3.04	0.45

Table 2: Random and drift velocity of the electrons. l = o.5 cm

cavity the T_e is still higher than the T_r or $(T_{ex})_r$ indicating that local thermodynamic equilibrium cannot be achieved in the microwave plasma.

4.1.3 Electron density (n_e)

Fig. 12 shows the electron density values as a function of pressure for the pure and mixed gases. In the pure gases, the electron density values are higher in CH_4 by almost one order of magnitude than in Ar, at the same distance from the antenna. The same effect can be seen in the electric conductivity values in Fig. 8. The reason for this effect is attributed to the contribution of electrons from the ionization of H, CH, CH_2, CH_3 instead of only from Ar in argon gas.

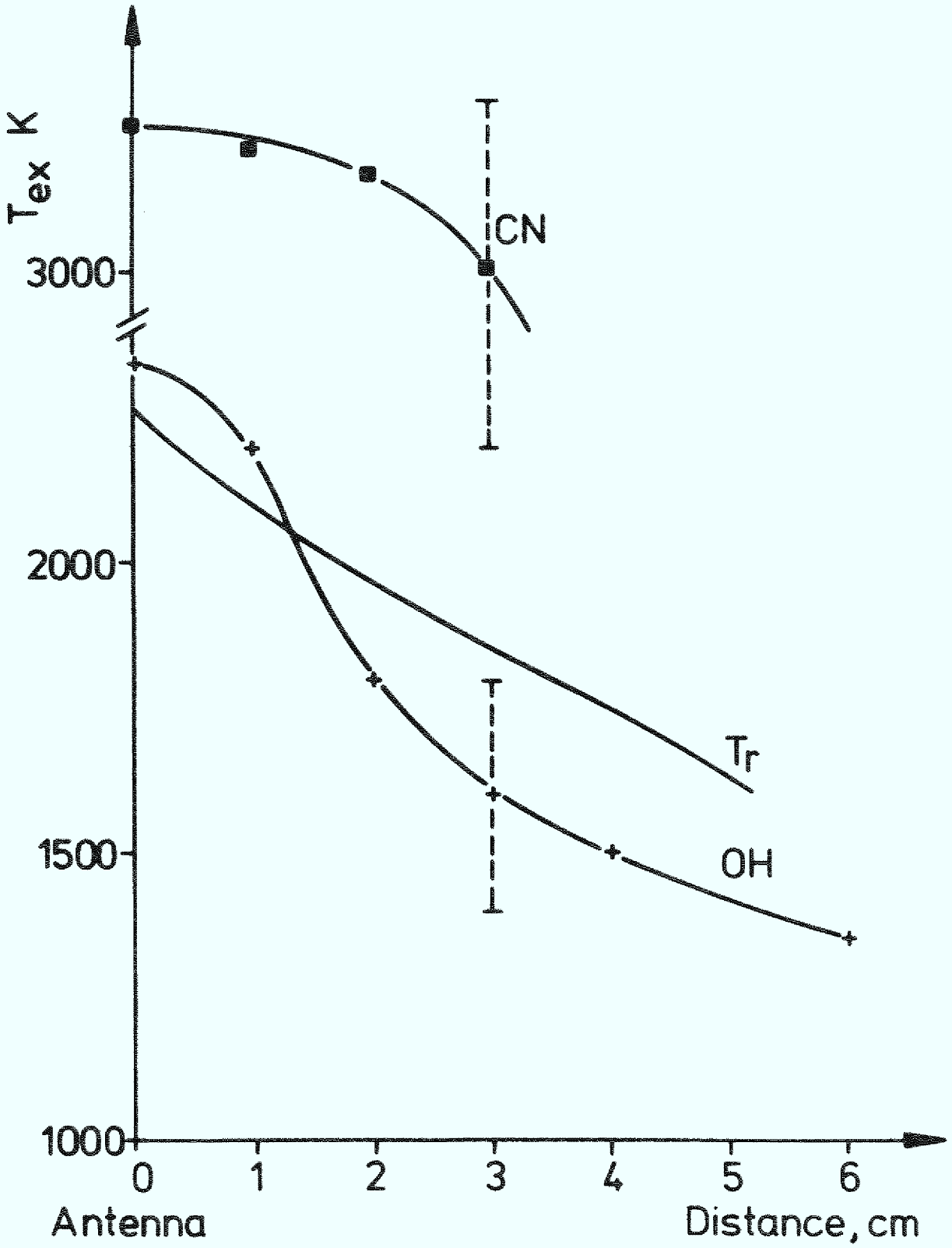

Fig. 11: "Excitation temperature" (CN) vibrational, (OH) rotational and (T1) reversal vs. distance from cavity center in methane.
(1.o torr; microwave power 12o W)

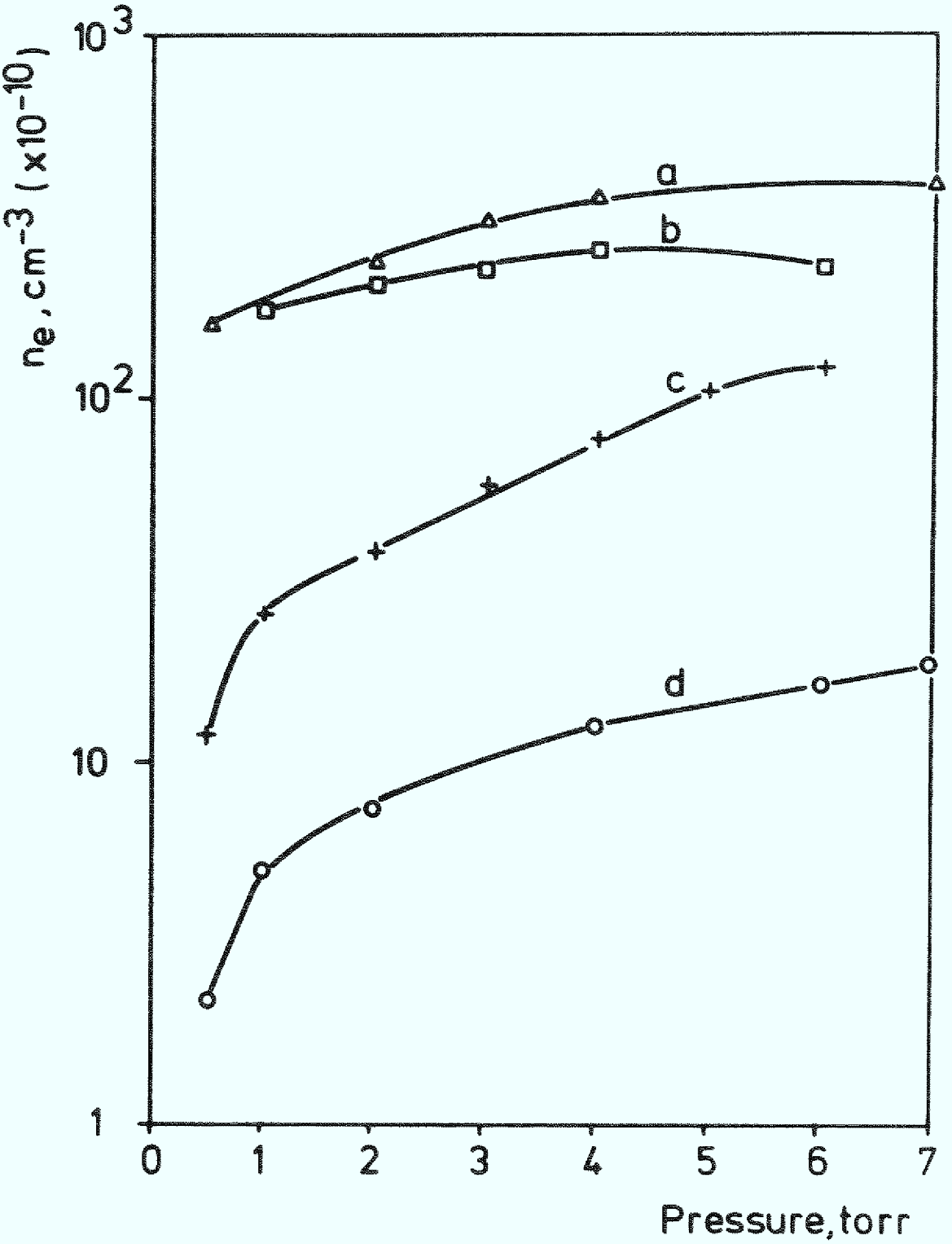

Fig. 12: Electron density vs. pressure. l = 1,3 cm. a = 2 torr CH_4 + varying Ar; b = 4 torr Ar + varying CH_4; c = CH_4; d = pure Ar.

Moreover, the ionization potential of molecules or radicals, such as, CH, CH_2, CH_3, is lower[29] than the ionization potential of argon. The addition of Ar to CH_4, or vice versa, increases the electron density when compared to the pure gases, by almost one order of magnitude at the same distance from the cavity center. This effect is primarily a result of the decrease in the electron drift velocity (see Table 2) at higher pressures (Fig. 12). The decrease in the electron drift velocity in the mixtures is easily understood from the values of the electron mean free path (λ_e) given in Table 3.

P Torr	E V cm^{-1}	T_e K	j_ex10^3 A cm^{-2}	v_ex10^{-5} cm s^{-1}	μ_ex10^{-5} cm^2 V^{-1}s^{-1}	σx10^4 Ω^{-1}cm^{-1}	n_ex10^{-10} cm^{-3}	$n_e v_e = n_i v_i$x10^{-15} cm^{-2}s^{-1}	v_ix10^{-3} cm s^{-1}	n_ix10^{-12} cm^{-3}	x10^2 λ_e cm
1.0	16.3	39,000	24.0	30.0	1.8	14.7	5.0	150.0	17.0	8.8	1.36
2.0	11.6	36,000	21.5	18.0	1.55	18.5	7.4	133.2	16.4	8.2	1.12
4.0	8.3	29,000	19.0	8.5	1.10	22.8	12.8	108.0	14.7	7.3	0.71
6.0	7.0	27,000	17.0	6.0	0.9	24.8	16.7	100.0	14.2	7.0	0.56
8.0	6.6	26,000	16.5	4.5	0.75	25.0	20.7	93.1	13.9	6.8	0.46
10.0	6.6	24,000	15.5	4.5	0.75	24.0	21.3	95.8	13.3	7.2	0.44

Table 3: Electric variables calculated from current-voltage plot of the floating double probes, W-probes; d=o.15 cm; l=1.3 cm; A_p=o.o48 cm^2; mw-12o W; reflected power 15 W - Argon -

Lower λ_e values at higher pressures indicates that the electrons have a higher probability to stay within the plasma instead of interacting with the walls; consequently, in CH_4-Ar mixtures, the electrons undergo more interactions with plasma particles than in each pure gas.
Returning now to Fig. 5, in which E values are given, one can explain why argon with its lower n_e value has the higher E value. Practically, the electron flux value $n_e(v_e)_d$,

is almost constant indicating a higher $(v_e)_d$ is required for lower n_e values. A higher probability of the electrons interaction with the walls is obtained at higher drift velocity values. The electrons interacting with the walls leave the plasma, and so the remaining ions in the plasma develop a higher space charge resulting with a higher electrostatic field (see also Fig. 8).

4.1.4 Ion density and ionization degree, α

Fig. 13 shows the variational total ion concentration in the plasma with pressure. The total ion concentration is the summation of H^+, CH_3^+, CH_2^+, and CH^+ ions in the CH_4 gas, and with Ar^+ ions in the gas mixtures. They were calculated from the general relationship $n_e(v_e)_d = n_i(v_i)_d$. The ion drift velocities for H^+, CH_3^+, CH_2^+, and Ar^+ were calculated separately using equation 3 and then summed. The results in Fig. 13 show that the highest ion concentration was found in the mixtures in which CH_4 pressure was varied in 4.o torr Ar. The ion concentration of each constituent of the pure gas is shown in Fig. 13 in which Ar^+ ions in argon reaches the highest value; within a factor of 2, the $n_{i(Ar^+)}$ is greater than $n_{i(CH_3^+,CH_2^+,CH^+)}$ and with about one order of magnitude $n_{i(Ar^+)}$ is greater than $n_{i(H^+)}$ in pure methane gas at the same pressures and microwave power. The higher value of $n_{i(Ar^+)}$ indicates that the ion interactions in CH_4 are greater than in argon. In other words, the products of the pyrolysis of CH_4 are interacting with the ions leaving a lower ion concentration to be measured, although the ionization potentials of these products are lower than argon's ionization potential. The last statement is more evident in the $n_{i(H^+)}$ value. If the pyrolysis of CH_4 produces C and $2H_2$ products, then the ion concentration of H^+ should be greater than the ion concentration of CH_3^+, CH_2^+ or CH^+. In reality, the $n_{i(H^+)}$ is by one order of magnitude lower than the $n_{i(CH_2^+}$, CH^+, etc.) .

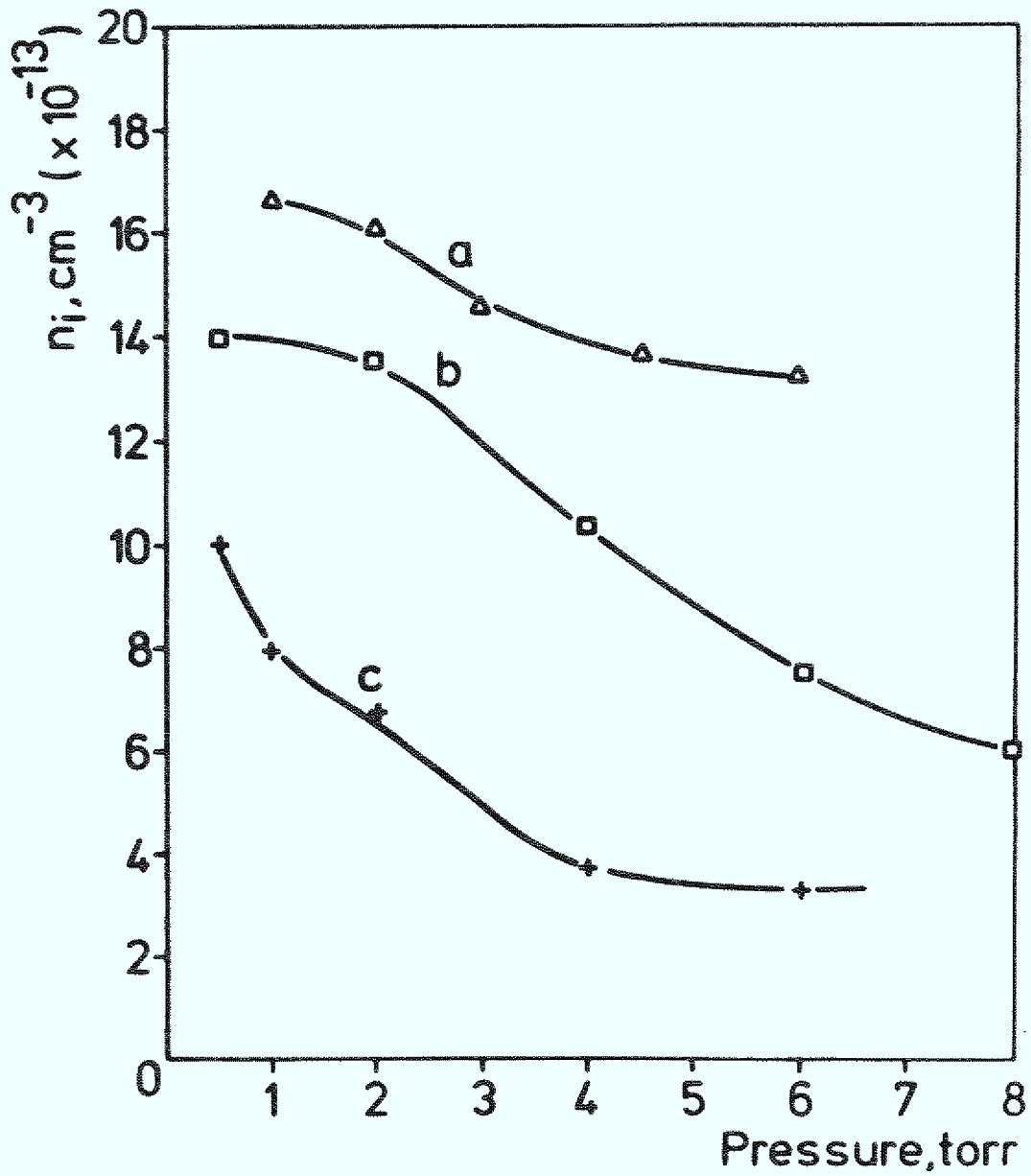

Fig. 13: Total ions concentration vs. pressure. a=4 torr Ar + varying CH_4; b=2 torr CH_4 + varying Ar; c=pure CH_4.

Fig. 14 showing that other chemical reactions, than the above one, occur in the pyrolysis of CH_4. Another indication for the chemical reactions occurring in the microwave plasma is in the decreasing values of $n_{i(CH_2^+, CH^+)}$

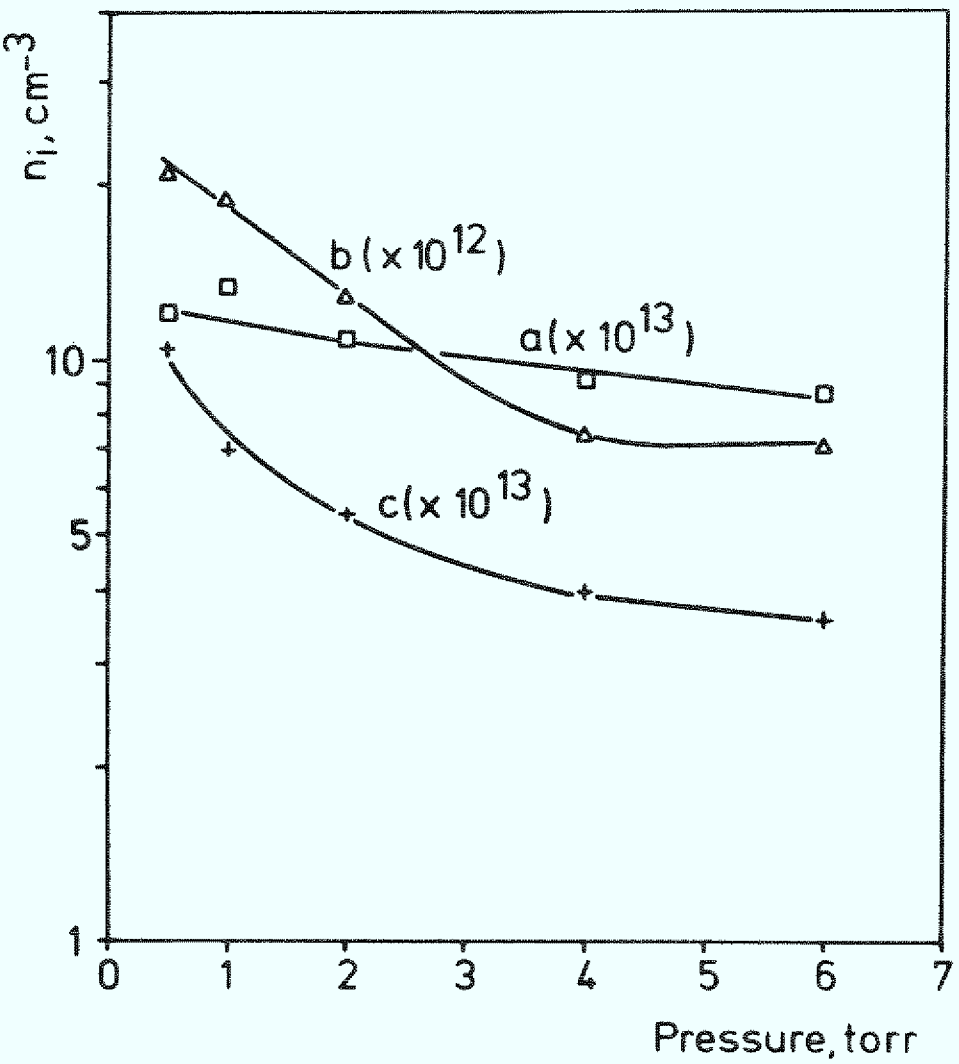

Fig. 14: Ion concentration in pure gases.
a=$n_i(Ar^+)/Ar$; b=$n_i(H^+)/CH_4$; c=$n_i(CH_2^+, CH^+...)/CH_4$.

and $n_{i(H^+)}$ with increasing CH_4 pressure, while $n_{i(Ar^+)}$ is almost constant with increasing pressure.
In the CH_4 and Ar mixtures, the total ion concentration decreases with increase of Ar/CH_4 pressure ratio. The different behaviour at 2 torr CH_4 with increasing Ar pressure is connected to the fact that Ar was added to the excited gases, i.e., part of CH_4 was already pyrolyzed.
The ionization degree (α) in the gas mixture was calculated and plotted vs ratio between the number of Ar particles and the number of CH_4 particles (in percent).

The $n_{i(Ar^+)}$ and $n_{i(CH_3^+,\ CH_2^+,\ CH^+)}$ in the gas mixture was calculated assuming their contribution to $(v_i)_d$ is due only to their molecular weight (see equation 3), i.e., they act as separate gases; the results of α given in Fig. 15 should be checked spectroscopically.
Fig. 15 shows a very marked trend of the CH_4 in the presence of argon; the ionization degree increases as the argon concentration increases. The ionization degree of Ar decreases by increasing CH_4 concentration.
The result of increasing ionization due to Ar was confirmed by the increase of the ionic spectral lines of CH^+ at 4225.3 Å and 3967.1 (R band heads for $\Delta v=0$ and $\Delta v=-1$ respectively). Furthermore, investigation is needed in order to understand the mechanism of the ionization of CH, CH_2... CH_3 etc., by argon.

4.1.5 Energy balance and steady state

Table 4 shows the changes in the values of electron temperature and density and ion concentration with time. The measurements of the double floating probes were taken after 1o, 3o, 6o, and 3oo s for the microwave plasma at various pressures. The results given in Table 4 indicate that the plasma at 1.3 cm from the antenna reaches a steady state after 12o-18o s.

In the theoretical consideration, the steady state is defined as being the equilibrium between the energy introduced and the energy dissipated by the microwave plasma. Using the "reversal temperature" from the energy balance, the mean electron density $\bar{n}_e$ was calculated. The $\bar{n}_e$ values given in Table 4 are higher by almost one order of magnitude than the electron density calculated from the floating probe measurements, indicating that no steady state was reached in the microwave plasma. On the other hand the $\bar{n}_e$ values are almost equal to the ion concentration n_i obtained from the probe measurements. If one assumes that the probes

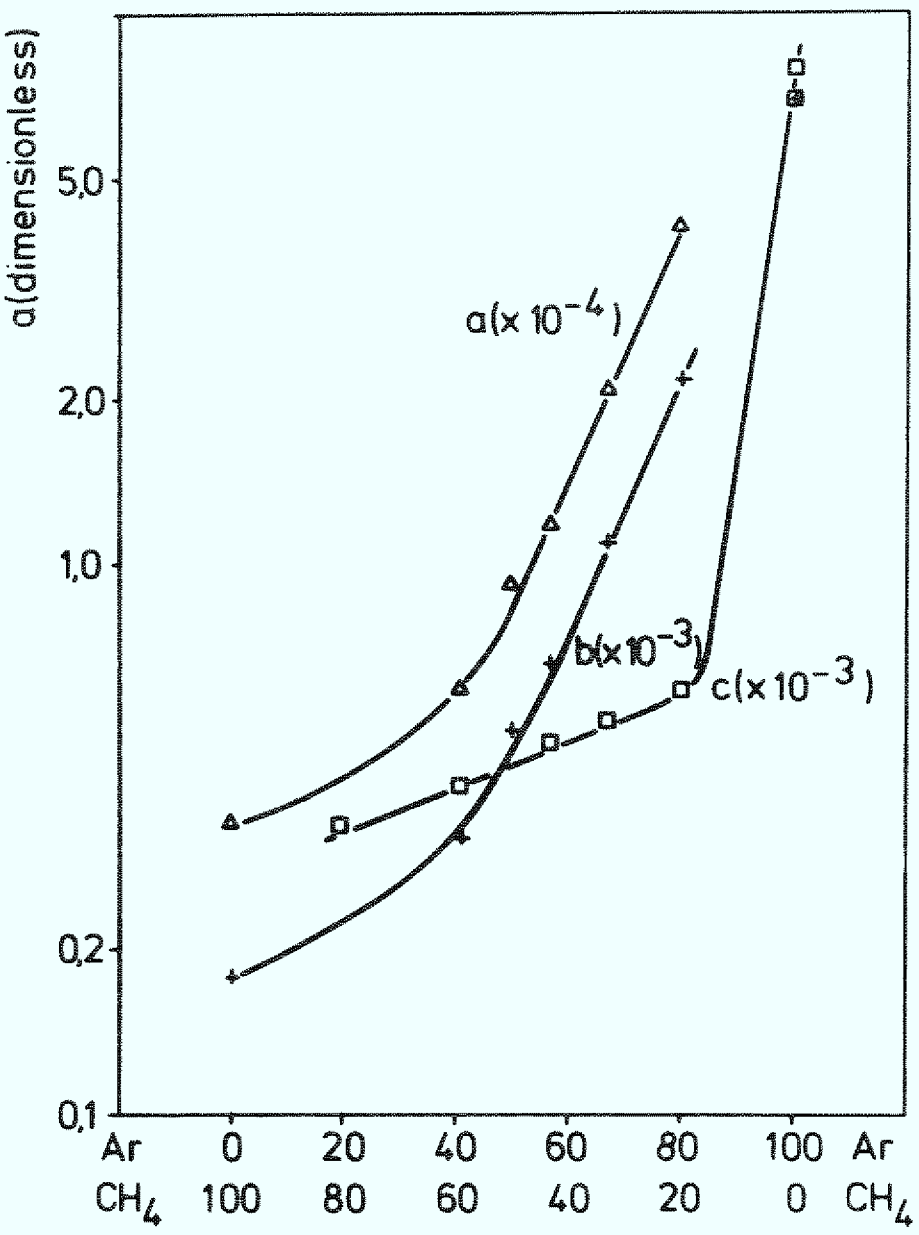

Fig. 15: Ionization degree (α) in gas mixtures.
Ar 4 torr + varying CH_4.
a=H ions; b=Ar ions; c=CH_2, CH ... ions.

P torr		t	$T_e x10^{-3}$	$j_e x10^{3}$	$n_e x10^{-12}$	$n_i x10^{-13}$	$\bar{n}_e x10^{-12}$ *
Ar	CH_4	s	K	A cm^{-2}	cm^{-3}	cm^{-3}	
4.0	1.0	10	37.0	24.5	1.80	18.5	16.2
		30	37.0	21.5	1.50	17.5	16.2
		60	32.0	19.0	1.20	16.4	9.6
		300	30.3	18.6	1.10	16.4	9.6
4.0	2.0	10	34.0	22.8	2.15	17.8	18.2
		30	31.0	18.6	1.70	15.3	18.2
		60	30.2	18.0	1.30	14.2	11.5
		300	29.6	17.6	1.20	14.1	11.5
4.0	4.0	10	31.5	21.0	2.60	17.3	21.5
		30	35.0	19.8	2.40	15.5	21.5
		60	29.6	15.0	1.50	12.1	14.1
		300	28.2	14.0	1.40	12.0	14.1

* Calculated from the energy balance equation.

Table 4: Microwave plasma variables with time.

cannot collect the negative ions which are formed as a result of electron affinities to molecules such as C_2, H_2, OH, CHO etc., then the positive ion concentration is equal with the summation of the densities of electron and negative ions. The presence of negative ions is indicated by the result $\bar{n}_e > n_e$. In that way, one fulfills the requirements for plasma electrical neutrality. The results obtained as function of time are probably due to the deposition of CH_4 pyrolysis particles on the tungsten probes. The steady state in the microwave plasma can be achieved by the addition of atoms or molecules with very low ionization potentials, such as Cs or K.

4.2 Emission measurements

4.2.1 Particle concentration

The emitting species from the microwave plasma with methane or methane-argon mixtures were measured densitometrically from spectrographic plates exposed through a 3.4 m grating spectrograph, Ebert type. The following species were detected: H, H_2, C, C_2, CH, and CH ions besides Ar and Ar ions spectra.
The aim in the emission measurement is the distribution of the particle concentration as a function of distance from the microwave cavity, microwave power and gas pressure. This aim was achieved by measuring spectral intensity ratios. If we consider, a given molecule, then the intensity J_1 of a specific spectral transition is given by:

$$J_1 = \left(\frac{h\nu_1}{4\pi}\right) A_1 \, n_{ex_1} \text{ erg cm}^{-3}\text{s}^{-1} \text{ sr}^{-1} \quad \ldots \qquad (21)$$

where A_1 is the transition probability of the spontaneous emission and $n_{ex_{j1}}$ is the particle concentration, cm^{-3}, populating the upper energetic level under consideration.

Assuming that the temperature is responsible for the population of the upper level then according to a Boltzmann distribution

$$n_{ex_1} = n_1 \frac{g_{ex_1}}{Z_1} \exp\left(-E_1/kT\right) \quad \ldots \qquad (22)$$

where g_{ex}, is the statistical weight of the upper level, Z_1 the partition function, n_1 the total concentration (atoms, molecules,ions) of the species j_1, E_{j1} the energy of excitation, k the Boltzmann constant, and T the gas temperature in (k).
For another species, 2, the J_2 and n_{ex_2} can be expressed analogously by Eqs. 21 and 22 with 2 instead of 1.
For the same temperature, the intensity ratio for the two particles 1 and 2 can be expressed as:

$$\frac{J_1}{J_2} = \frac{\nu_1}{\nu_2} \frac{(g_{ex}A)_1}{(g_{ex}A)_2} \frac{n_1}{n_2} \frac{(1-\alpha)_1}{(1-\alpha)_2} \exp\left(-\frac{1}{kT}(E_1-E_2)\right) \qquad (23)$$

where α is the degree of ionization for the given species.

Another factor ß should be taken into account which indicates the degree of dissociation for a given molecule to its components.
Now if one uses the intensity ratios for species having similar excitation potentials (within ≈ o.5 eV), then the exponent term in Eq. (23) has a value near unity. For example, the excitation energies for CH, C_2, and H_2 are between 3 and 3.4 eV. Furthermore, the dissociation energies for these species are between 3.5 and 6 eV[36], while the ionization potentials of these molecules are between 4.1 and 5.5 eV[36]. In this case, Eq. (23) can be further simplied taking the ratios $(1-\alpha)_1/(1-\alpha)_2$ and $ß_{j_1}/ß_{j_2}$ to be near unity.

For species like CH, C_2, and H_2 using the above simplifications, Eq. 23 will have the following form:

$$\frac{J_1}{J_2} \approx \frac{(\nu gA)_1}{(\nu gA)_2} \frac{n_1}{n_2} \frac{Z_2}{Z_1} \quad \ldots \qquad (24)$$

In the case of atoms like C and H which have about 5 eV excitation energies Eq. 23 should be used instead of Eq. 24. From the relative intensity measurements and using the known data for all other parameters, the ratio n_1/n_2 is calculated and plotted vs. microwave power, gas pressure, and distance from the microwave cavity.

4.2.2 n_1/n_2

Figures 16 and 17 show typical intensity ratio normalized to the intensity of C_2 (Fig. 16) and to the intensity of CH (Fig. 17), as a function of methane pressure. The following ratios of particle concentration were calculated: n_{CH}/n_{C_2}, n_{H_2}/n_{C_2}, and n_{H_2}/n_{CH} using Eq. (24) while the other n_H/n_{C_2}, n_C/n_{C_2}, n_H/n_{CH} were calculated using Eq. (23). Furthermore, the ratio n_{CH^+}/n_{CH} was calculated using the Saha relationship for ionic and atomic spectral line.

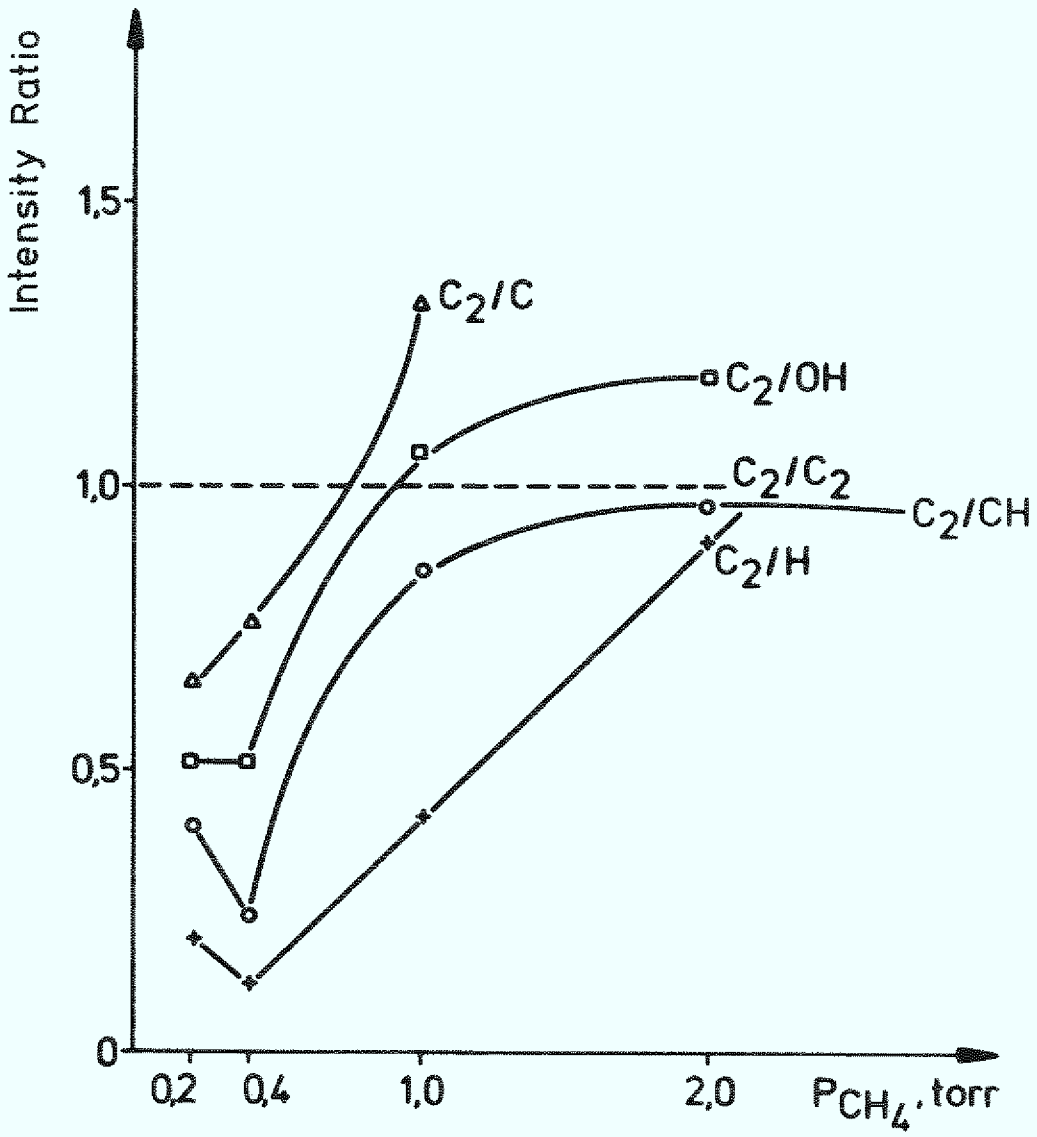

Fig. 16: Intensity ratio vs. pressure (CH_4)
Microwave 1ooW; volume ~ 15 cm^3; 1oo s exposure.

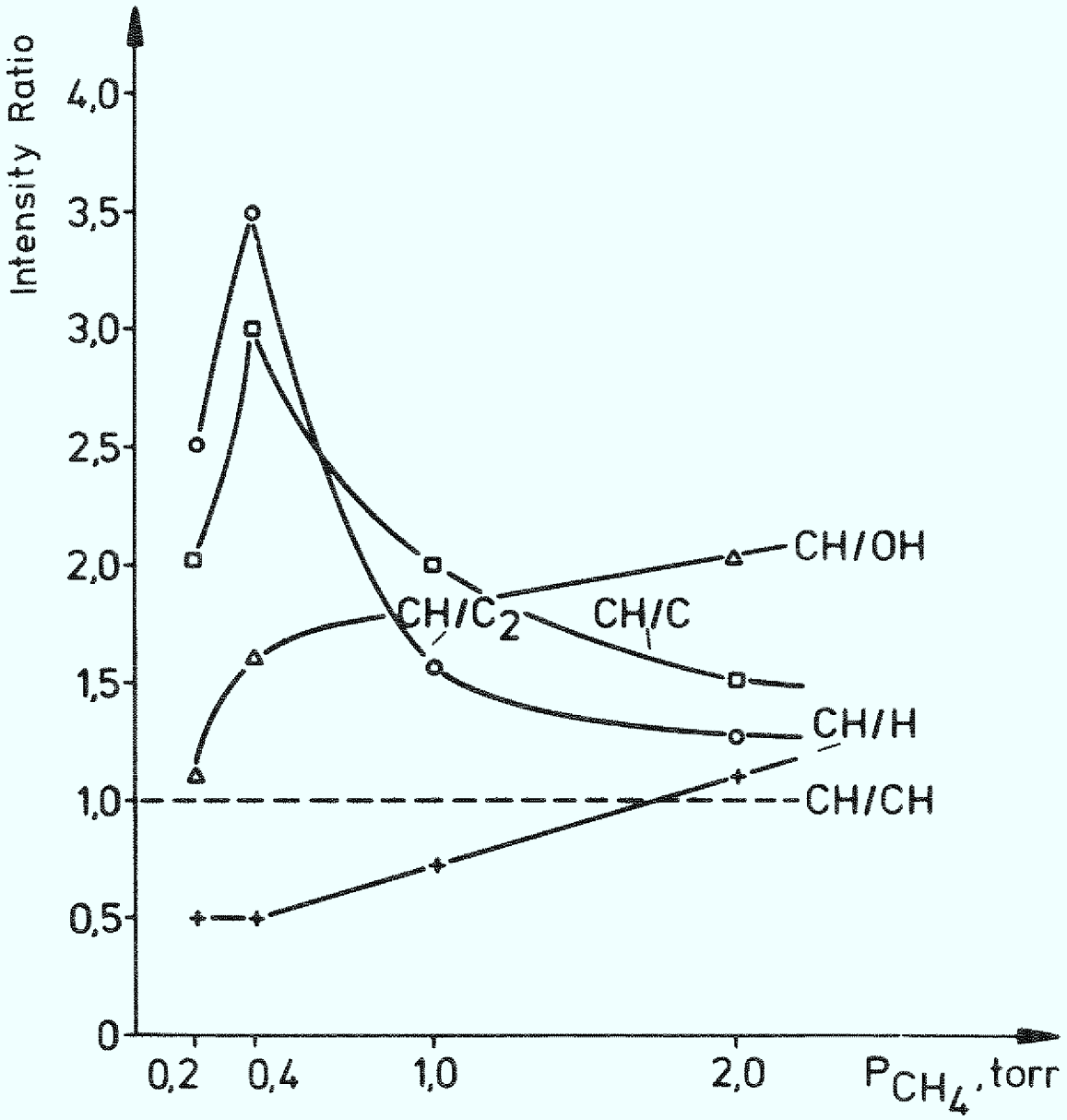

Fig. 17: Intensity ratio vs. pressure (CH_4). Microwave 100 W; volume ~15 cm^3; 100 s exposure.

Table 5 shows the particle concentration ratio when the pressure of methane and methane-argon was varied. The wavelength used for the intensity measurements are indicated in Table 5. Increasing gas pressure, the concentrations of H and C atoms are reduced while the concentrations of radicals such as C_2, CH are enhanced.

Pressure		n_1/n^a_2								
CH_4	Ar	CH/C_2	H_2/C_2	H_2/CH	H/C_2	C/C_2	H/CH	C/CH	CH^+/CH	H/H_2
torr										
0.5		2.5	8.0	3.0	5.0	1.3	2.0	0.5	0.3	0.3
1.0		4.0	10.0	3.0	7.0	1.0	1.5	0.3	0.4	0.4
2.0		4.0	11.0	3.5	3.0	0.7	0.8	0.2	0.1	0.4
4.0		4.0	12.0	3.5	2.0	0.2	0.5	0.1	0.07	0.5
2.0	1.0	2.0							0.8	0.7
2.0	2.0	3.0							1.0	0.8
2.0	4.0	3.0							1.2	1.0
2.0	6.0	3.0							1.2	1.0
2.0										

[a] Wavelengths used:

CH	3889 Å
C_2	4737 Å
H	4101 Å
C	2478 Å
CH^+	4225 Å
H_2	5420 Å

Table 5: Particle concentration ratio vs. gas pressure.
MW 100 W, center of cavity
Spectrographic Plates SA-1; SA-3; N1 "KODAK"

Exposing the center of the microwave cavity to the spectrograph at 4.0 torr CH_4, the molecule having highest concentration is H_2 and the next highest are the CH and C_2 radicals. Assuming formation of higher molecular weight hydrocarbon in the pyrolysis of methane, the high concentration of H_2 results in the formation of unsaturated hydrocarbons.

The presence of Ar in the pyrolysis of CH_4 by microwaves enhanced the ion formation as shown in Table 5. The concentration of CH radical is assumed to be constant. Another effect observed in the presence of Ar is the small increase of H atoms in comparison with H_2. The ionization effect observed in emission measurement is in agreement with the result obtained from the double floating probes.

More information about the hydrocarbon formed in the pyrolysis of CH_4 and the concentrations of other molecules is needed. The emission measurements does not provide this information as no other hydrocarbon molecules are detected.

Table 6 shows the particle concentration ratio of several species with respect to the distance from the center of the microwave cavity. It should be noted that at a distance of 3.o cm the emission spectrum of the atomic species is almost non-existent even at large exposures (up to 5 minutes), for a CH_4 pressure of 4.o torr. This result is consistent with Fig. 11 indicating a cooler plasma. Nevertheless the emission of the molecular species, C_2, CH, and H_2 was detected at this distance. As shown in Table 6, the concentration ratio of C_2/CH, H_2/CH, and H_2/C_2 have valuesnear unity. In other words, the concentration of C_2, CH, and H_2 have the same value. The interpretation of this result is difficult due to the shrinkage of the microwave plasma at higher CH_4 pressure. Having a cooler plasma, one may expect a smaller production of C_2, H_2, and CH, i.e., less fragmentation of the CH_4 molecule. On the other hand, the smaller concentration of C_2 and CH radicals indicates their reactions with methane to form higher hydrocarbons.

Pressure torr		n_1/n_2									
		1.0 cm				2.0 cm			3.0 cm		
CH_4	Ar	CH/C_2	H_2/C_2	H_2/CH	H/H_2	CH/CH_2	H_2/C_2	H_2/CH	CH/CH_2	H_2/C_2	H_2/CH
2.0		3.0	11.0	4.0	0.2	2.0	3.0	1.0	0.9	1.0	0.8
4.0		2.0	3.0	2.0	0.1	1.0	1.0	1.0	0.9	0.8	0.7
2.0	2.0	2.0				1.0			0.8		
2.0	6.0	0.9				1.0			0.9		

Table 6: Particle concentration ratio vs. distance from the center of the microwave cavity. MW 1oo W

Table 7 shows the n_1/n_2 ratio with respect to microwave power, where measured in the center of the cavity. Upon increasing the power from 6o up to 12o W, no differences in the n_1/n_2 ratio were detected.

Pressure torr		n_1/n_2									
		60 W			80 W			120 W			
CH_4	Ar	CH/C_2	H_2/C_2	H_2/CH	CH/C_2	H_2/C_2	H_2/CH	CH/C_2	H_2/C_2	H_2/CH	CH^+/CH
2.0		3.0	12.0	4.0	4.0	12.0	5.0	4.S	11.0	3.5	0.3
4.0		4.0	11.0	3.0	5.0	12.0	3.0	5.0	10.0	3.0	0.3
2.0	2.0	2.0			3.0			4.0			1.0
2.0	6.0	1.5			2.0			3.0			1.0

Table 7: Particle concentration ratio vs. microwave power. At center of microwave cavity.

4.3 Absorption

In each of the three systems, the absorption spectrum for a given microwave plasma, with regard to the CH_4 pressure or flow, was normalized. The normalization is the ratio between the light absorbed by the CH_4 pyrolysed by the microwave to that the CH_4 without the microwave. In this way, a normalized coefficient of absorption (k_ν) for each radical and excited molecule formed in the pyrolysis of CH_4 was evaluated.
The results are given and discussed separately for each system.

4.3.1 The Afterglow system

Table 8 shows the normalized absorbance obtained for the CH_3 radical. Using the 5 optical passages of the light from the Xe lamps, in the afterglow system, only the CH_3 radical has been detected, at 2157 and 2163 Å. No other radicals or molecules were detected in this system. The values given in Table 1 indicate a small amount of CH_3 is present in the afterglow region, the absence of the other species is connected to the lifetime of the other radicals. A distance of 2.o cm from the center of the cavity to the measured region in the afterglow is too great to allow measurement of other radicals. Accepting Herzberg's[35] value of ~5o μs as the lifetime of the CH_3 radical, radicals, such as CH_2, C_2H_2, C_5H_5 or others, have a shorter lifetime than CH_3.To estimate the minimum distance in order to measure the absorption of other radicals is very difficult because no data are available on the lifetime of the other radicals.

Molecule	λ Å	$k_\nu \ell$ (dimensionless)							
		System 1				System 2			
		CH_4	Ar/CH_4			CH_4	Ar/CH_4		
			1.0	1.5	2.0		1.0	1.5	2.0
CH_3	2157	0.28	0.2	0.16	0.12	0.4	0.35	0.3	0.2
	2163	0.21	0.15	0.12	0.12	0.35	0.28	0.25	0.15
C_2H_2	2285	-	-	-	-	0.19	0.12	-	-
	2288	-	-	-	-	0.19	0.12	-	-

Table 8: Normalized absorbance of CH_3 and C_2H_2 in systems 1 & 2.
2.o torr CH_4; 8o W microwave power.

Another unsatisfactory result is that molecules such as C_2H_2 or C_6H_6 have not been detected in absorption. This result can be interpreted by: i) either the concentration of such molecules is too small to be detected in absorption, and so the 5 passages of source radiation are insufficient, or ii) the molecules being in their excited states react with other particles in time periods shorter than 5o μs. Now if the last possibility is the real process taking place in the CH_4 pyrolysis, then, even in a flow system, the above molecules would not be detected in absorption. On the other hand, if the first possibility is the adequate one, then these molecules will be detected in the flow system where the molecules are formed "in situ" from the pyrolysis of CH_4.
The presence of Ar in the pyrolysis of methane did not affect the absorption spectrum of CH_3.

4.3.2 The "Non-Flow" system

In this case, the light from the Xe lamp is passed only once through the microwave plasma.
Table 8 shows the normalized absorbance values for the CH_3 radical and the C_2H_2 molecule. Besides them, no other radicals or molecules were detected in this system. As compared with the afterglow system, the values of the normalized absorbance for CH_3 are almost the same. The presence of the C_2H_2 molecule (measured by absorption) could be explained by the motion of methane molecules. In other words, due to processes such as convection and diffusion, fresh CH_4 from the surrounding atmosphere penetrate into the microwave plasma, pyrolyzing and forming a higher concentration, C_2H_2 could be detected in absorption.
The presence of Ar in the methane pyrolysis has an inhibitory effect on the absorbance of CH_3 and C_2H_2; lower values were found for CH_3 radical and no acetylene was detected when argon was added to the methane (Table 8). The maximum inhibition effect was obtained at pressure ratio

Ar/CH_4 = 2. As mentioned in the previous sections of this report, the presence of Ar in the pyrolysis of CH_4 increases the ionization of the particles in the microwave plasma. Due to this effect, the C_2H_2 molecule as well as the CH_3 radical are partially ionized, lowering the concentrations in their neutral ground states, resulting in a decrease of absorbance.
The measurements of absorption by the two systems and the formation of CH_3 radicals in the pyrolysis of methane by microwaves indicate, that in a flow system, more radicals and molecules could be detected and analyzed by absorption techniques.

4.3.3 The Flow system

Fig. 18 shows the absorption spectrum obtained by only one passage of the source radiation when CH_4 alone flowed through the microwave discharge. In a spectral range 2000-2400 Å, the following radicals and molecules were measured in absorption: C_2H_4, CH_3, CO, C_2, N_2, C_4H_2, C_2H_5, C_2H_2, C_5H_5 and C_6H_6. The CO and C_2N_2 bands are probably due to the presence of CO and N_2 as impurities in methane. At wavelengths higher than 3400 Å, some unidentifiable absorption peaks appeared; these are not included in this progress report.
Thehighest normalized absorbance was obtained for the CH_3 radical indicating that this radical was produced (by pyrolysis) in the highest concentration compared to the other molecules produced and detected. The absorption bands of CH_3 at 2157, 2163, and 2188 Å (the weakest 2202 Å band is probably overlapped by the C_4H_2 band) are best defined spectrally as compared with the other radicals and molecular spectral bands. Besides CH_3, the other molecular absorption bands are weaker and poorly defined[36]. Normalized absorption peaks of a number of species were obtained, as shown in Fig. 18; theses molecular species were formed in the pyrolysis of CH_4 by microwaves.

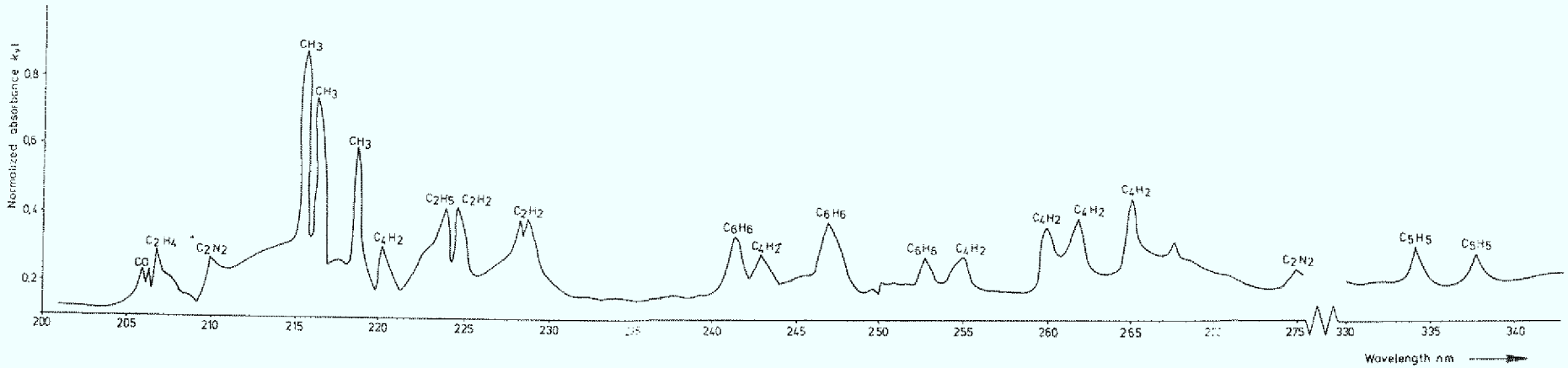

Fig. 18: Normalized absorbance vs. wavelength at 1,5 torr CH_4.
Flow system; CH_4 flow $\sim$ 35 ml/min; 80 W microwave power.

Gaydon et al.[32] has provisionally assigned the band heads at 2220 and 2242 Å to the C_2H_5 radical; the same uncertainty is valid on our assignment to this radical. As far as the assignment of the other spectral bands, their validity is as expressed in the literature[31-36].

Fig, 19 shows the increase of the absorbance of CH_3 at 2157 Å with increase in the methane pressure in the system. In other words, more CH_4 produces more CH_3 radicals in the microwave discharge. Almost twice as many methyl radicals were produced by increasing the methane pressure from 1.0 to 5.0 torr. The same behaviour was obtained for all the spectral bands of the various radicals and molecules reported in Fig. 18.

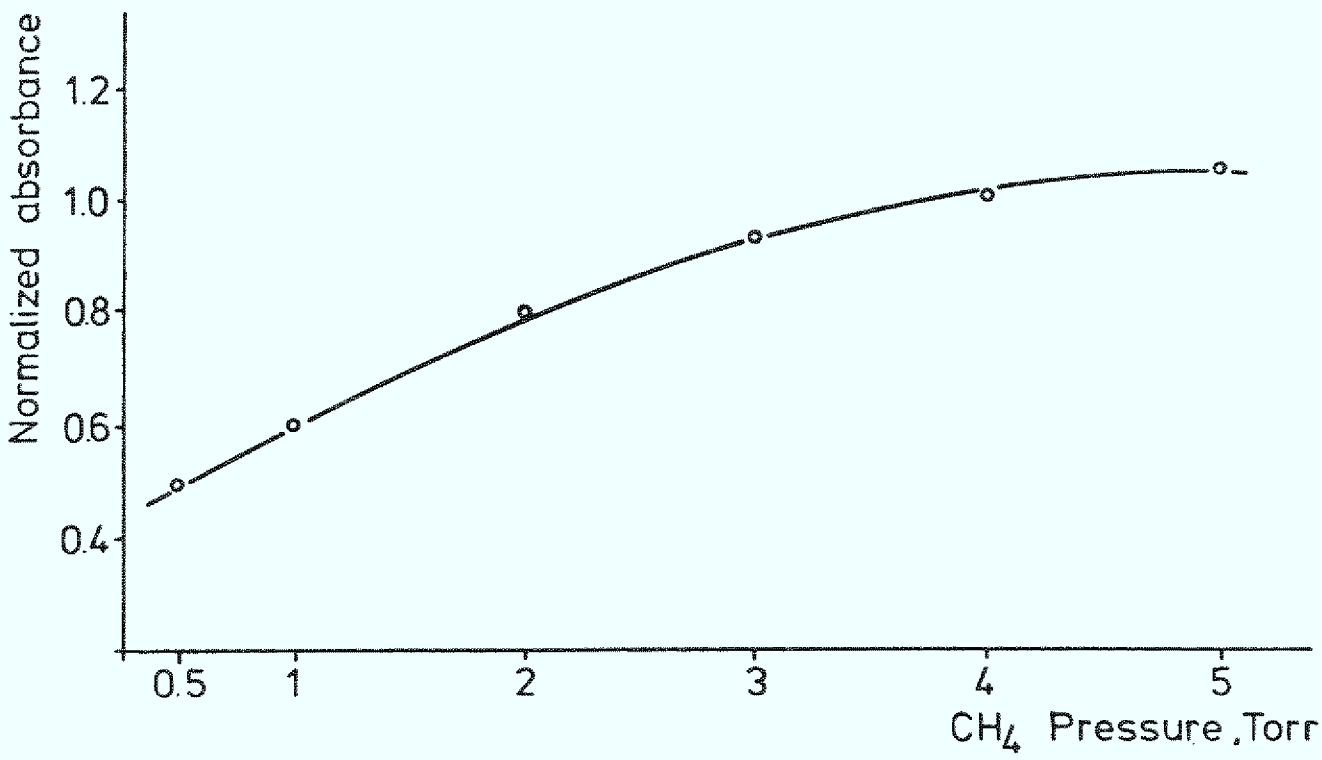

Fig. 19: Variation of absorbance with methane pressure. Flow system; CH_3=2157 Å; 80 W microwave power.

The presence of argon in the microwave plasma of methane inhibits the absorbance of each molecular band. This inhibition is attributed to the ionization effects of argon on the molecular species. Based on the ionization potential given by Herzberg[34] for the CH_3 and CH_2 radicals as 79392 and 83857 cm^{-1}, respectively, one can assume that the excited argon states, in particular argon metastable states ($\sim$93ooo cm^{-1}) by collisions with these radicals will partially ionize them. The absorbance was reduced by 5o% in an argon-methane mixture containing up to 3 parts Ar to each part CH_4. The increase of argon concentration above the Ar/CH_4 ratio of 3 does not affect the absorbance. The band heads measured in absorption in mixtures of 3:1 argon to methane were those of CH_3, C_2H_5, C_2H_2, and C_3H_2 (Fig. 18). The band heads of C_6H_6 and C_5H_5 were completely depressed. Due to the presence of impurities in argon, such as O_2 and N_2 the spectral absorbance of CO and C_2N_2 was enhanced in the Ar-CH_4 mixtures. Their enhancement was found to be proportional to the increase of Ar in the gas mixture.

The normalized absorbances given in Table 8 and Figs. 18 and 19 should lead to the calculation of the concentration of each molecule and radical if the following are known:

i) The vibrational transitions from the ground electronic state to the excited states.

ii) The transition probability for absorption and the statistical weights of each state; in other words, the oscillator strengths of the spectral transitions.

For the majority of the molecular absorption spectra obtained from the pyrolysis of methane, neither (i) nor (ii) are known or well-established [31-35]. Moreover, due to the weak absorption spectrum, the confidence of each molecular assignment is relatively low, in particular for the ethyl radical. Based upon the pressure in the system, the estimated life time of the CH_3 radical and the path length of about 5.o cm in the microwave discharge, one can put an upper limit to the CH_3 pressure as about o.oo2 torr[31,36]. An estimation of the CH_3 concentration in the microwave plasma can be obtained using the relationship

$$\int k_\nu d\nu = \frac{\lambda_o^2}{8\pi} \frac{g_2}{g_1} \frac{n}{\tau} \qquad (25)$$

Where $\int k_\nu d\nu$ is the integrated coefficient of absorption, λ_o is the wavelength in Å, n the particle concentration, cm^{-3}, and the lifetime of the transition, in s. Using the value of $\int k_\nu d\nu$ from Fig. 4 for CH_3 at 2157 Å and assuming g_2/g_1, the statistical weights to be unity, one obtains $n_{CH_3} \approx 10^{12}$ particles in one cm^3 of the microwave plasma. In other words, the concentration of the CH_3 radical must have been no more than one in 1000 for a methane pressure of 1.5 torr. From Fig. 18 and continuing this approximate calculation, one obtains for the other radicals and molecules a concentration of about one in 5000 at 1.5 torr methane. From these approximate calculations and based on the reasons (i) and (ii) mentioned above, one cannot investigate the kinetics of CH_4 pyrolysis from only the absorption spectrum.

5. Remarks for Future Work

The direct result in this work is that the pyrolysis of methane by microwaves leads to the formation of various radicals. These radicals can react with each other or with other molecules formed by the pyrolysis or with the non-pyrolyzed CH_4 moleclues in order to form the final pyrocarbon molecule. The kinetic studies leading to the rate determining steps in the formation of pyrocarbon, from only the absorption spectra obtained in this work, is almost impossible due to the unavailable spectral data for the heavier hydrocarbon molecules. The use of a quadrupole mass spectrometer coupled to the microwave plasma of CH_4 will lead to the identification of more heavier hydrocarbons in their excited states, thus allowing the kinetic studies for the rate determining steps in the pyrocarbon formation.

APPENDIX

Justification of assumption $n_e(v_e)_d = n_i(v_i)_d$

According to Condon and Odishaw[39], the equality between the flow rates of positive ions and electrons occurs for ambipolar diffusion. For the ambipolar diffusion case, the following equations for each flow rate are given:
For ions:

$$n_i v_i = -D_i \nabla n_i + \mu_i E n_i; \qquad (A1)$$

and for electrons:

$$n_e v_e = -D_e \nabla n_e - \mu_e E n_e; \qquad (A2)$$

where D_i and D_e are the coefficient of diffusion of ions and electrons, respectively. Dividing each equation by $n_i \mu_i$ and $n_e \mu_e$, respectively, one obtains:

$$v_i / \mu_i + \frac{D_i}{\mu_i} \frac{\nabla n_i}{n_i} = E$$

$$v_e / \mu_e + \frac{D_e}{\mu_e} \frac{\nabla n_e}{n_e} = E.$$

Since $\mu_e > \mu_i$, the condition for the equality of fluxes in ambipolar diffusion requires that $v_e > v_i$. At the gas temperature, where $D_e / \mu_e = E_i / \mu_i = kTr/e$, the equality between Eqs. (A1) and (A2) is reached only

$$\frac{\nabla n_e}{n_e} \approx \frac{\nabla n_i}{n_i}.$$

Assuming a very small gradient for both ions and electron concentration

$$\left(\frac{\nabla n_e}{n_e} = \frac{\nabla n_i}{n_i} = 1 \right)$$

and using the data of the reversal temperature and electric field strength, one obtains for a pressure of 2.0 torr Ar

for example:

$$v_i / \mu_i = - o.19 + E; \qquad (A3)$$

and

$$v_e / \mu_e = - o.19 + E. \qquad (A4)$$

With $E \tilde{=} 14.5$ V cm^{-1}, the electric field strength in the above equations is the dominant value, (even for $T_e \gg T_i$ at $D_e / \mu_e = 3.7$) resulting that for a microwave plasma at low pressure of Ar, the ion and electron velocities are in fact their respective drift velocities, namely $(v_i)_d$ and $(v_e)_d$ [31].

Returning to the equality of fluxes, it is evident that:

$$(v_i)_d n_i = (v_e)_d n_e \qquad (A5)$$

References
==========

1.) H.F. Calcote: 8th Sym. Combustion, p. 184, Baltimore Williams and Wilkins (1962)

2.) H.F. Calcote: 9th Symp. Combustion, p. 132, New York Academic Press (1963)

3.) D.E. Jensen and S.C. Kurzius: Combustion Flame 13, 219 (1969)

4.) D. Bradley and K.J. Matthews: 11th Sym. Combustion, p. 359, Pittsburgh Combustion Inst. (1967)

5.) R.M. Clements and P.R. Smy: J.App.Phys. 44, 355o (1973)

6.) A.G. Gaydon and H.G. Wolfhard: Flames, Their Structure, Radiation and Temperature, Chapman and Hall, London (196o)

7.) B.E.L. Travers and H. Williams: 1oth Sym. Combustion, p. 657, Pittsburg Combustion Inst. (1965)

8.) J. Lawton and F.J. Weinberg: Electrical Aspects of Combustion, Clarendon Press Oxford (1969)

9.) R. Avni: Spectrochim. Acta, 23B, 597 (1968)

1o.) W. Finkelnburg and H. Maecker: Handbuch der Physik, 22, 254, Springer Verlag, Berlin (1956)

11.) J.D. Swift and M.J.R. Schwar: Electrical Probes for Plasma Diagnostics, Elsevier, N.Y. (1969)

11a) W.P. Allis and D.J. Rose: Phys. Rev. 93, 84 (1954)

12.) J. Polman: Physica 34, 31o (1967)

13.) B.E. Keen and W.H.W. Fletcher: J. Phys. D. (Appl.Phys.), 4, 1695 (1971)

14.) M.A. Heald and C.B. Wharton: Plasma Diagnostics with Microwaves, J. Wiley & Sons, N.Y. (1965)

15.) L. Schott: Plasma Diagnostics, Ed. W. Lochte-Holtgreven Chap. 11, North Holland Pub. Co., Amsterdam (1963)

16.) E.O. Johnson and L. Malter: Phys. Rev., 8o, 58 (195o)

16a) J.A. Smit: Thesis (in Dutch), Univ. Utrecht (1951)

17.) W. Elenbaas: Physica 1, 673 (1934)

18.) G. Heller: Physica 6, 389 (1935)

19.) G. Francis: Ionization Phenomena in Gases, Butterworths, London (196o)

2o.) P.W.J.M. Boumans: Theory of Spectrochemical Excitation, Hilger and Watts, London (1966)

21.) R.L. Roes: Thesis (in Dutch) Univ. Utrecht (1962)

22.) R. Avni and F.S. Klein: Spectrochim. Acta, 28B, 319 (1973)

23.) Landolt-Börnstein: Zahl. Funktionen IV Band, 3 Teil, p. 97, Springer Verlag, Berlin (1957)

24.) N.E. Bradbury and A.A. Nielsen: Phys. Rev. 49, 388 (1936)

25.) N. Russel and A.A. Nielsen: Phys. Rev. 5o, 95o (1936)

26.) G.H. Dieke and H.M. Crosswhite: J. Quant. Spectrosc. Rad. Transfer, 2, 97 (1962)

27.) W. Snelleman: Thesis Univ. Utrecht (1965)

28.) V. Vujnović: J. Opt. Soc. Am. 6o, 177 (197o)

29.) G. Herzberg: The Spectra and Structure of Simple Free Radicals, Cornell Univ. Press, Ithaca (1971)

3o.) L. Sütterlin: KFA-Report Jül-735-RW (1971)

31.) G. Herzberg: Spectra of Diatomic Molecules, Von Nostrand Co. Canada (195o)

32.) A.G. Gaydon, G.N. Spokes and J. von Suchtelen: Proc. Roy. Soc., 256A, 323 (196o)

33.) P.G. Wilkinson and R.S. Mulliken: J.Chem. Phys. 23, 1895 (1955)

34.) B.A. Thrush: Nature 178, 155 (1956)

35.) G. Herzberg: Proc. Roy. Soc., 262A, 291 (1961)

36.) R.W.B. Pearse and A.G. Gaydon: The Identification of Molecular Spectra, Chapman and Hall, London (1965)

37.) G. Herzberg and J. Shoosmith: Can. J. Phys. 34, 523 (1956)

38.) A.G. Gaydon: Dissociation Energies, Chapman and Hall, London (1968)

39.) E.V. Condon and H. Odishaw: Handbook of Physics, p. 4-159 to 165 McGraw Hill, N.Y. (1958)